Use of the Normalized Hydrophilic-Lipophilic-Deviation (HLD$_N$) equation for determining the Equivalent Alkane Carbon Number (EACN) of oils and the Preferred Alkane Carbon Number (PACN) of nonionic surfactants by the Fish-Tail Method (FTM)

Jean-Marie Aubry,[a]* Jesus Fermin Ontiveros,[a] Jean-Louis Salager,[b] Véronique Nardello-Rataj[a]

[a] Univ. Lille, CNRS, Centrale Lille, ENSCL, Univ. Artois, UMR 8181 - UCCS

Unité de Catalyse et Chimie du Solide, F-59000 Lille, France

[b]Laboratorio FIRP, Ingeniería Química, Universidad de Los Andes, Mérida 5101, Venezuela

Abstract

The standard HLD (Hydrophilic-Lipophilic-Deviation) equation expressing quantitatively the deviation from the "optimum formulation" of Surfactant/Oil/Water systems is normalized and simplified into a relation including only the three more meaningful formulation variables, namely *(i)* the "Preferred Alkane Carbon Number" PACN which expresses the amphiphilicity of the surfactant, *(ii)* the "Equivalent Alkane Carbon Number" EACN which accurately reflects the hydrophobicity of the oil and *(iii)* the temperature which has a strong influence on ethoxylated surfactants and is thus selected as an effective, continuous and reversible scanning variable. The PACN and EACN values, as well as the "temperature-sensitivity-coefficient" τ of surfactants are determined by reviewing available data in the literature for 17 nonionic *n*-alkyl polyglycol ether (C$_i$E$_j$) surfactants and 125 well-defined oils. The key information used is the so-called "fish-tail-temperature" T* which is a unique data point in true ternary C$_i$E$_j$/Oil/Water fish diagrams. The PACNs of C$_i$E$_j$ surfactants are compared with other descriptors of their amphiphilicity, namely, the cloud point, the HLB number and the PIT-slope value. The EACNs of oils are rationalized by the Effective-Packing-Parameter concept and modelled thanks to the COSMO-RS theory.

Keywords: HLD (Hydrophilic-Lipophilic-Deviation); EACN (Equivalent Alkane Carbon Number); PACN (Preferred Alkane Carbon Number); Optimum formulation; Fish diagram; Cloud point; COSMO-RS

Contents

1 Introduction

In the past century a large variety of surfactants have been developed for offering a wide range of functionalities including: surface or interfacial tension reduction, surface wetting modification, emulsification / demulsification, foaming/defoaming, dispersion stabilisation / breaking, tuning of rheological profile and solubilisation within micelles, microemulsions or liquid crystals. Actually, surfactants are key ingredients in various complex end-use products containing a high number of components. This results in a huge number of variables that must be adjusted to optimize the formulations performances. As a consequence, formulation is often perceived as an art rather than a science, since the development of an effective recipe requires laborious trial-and-error experimentations to build up a practical know-how [1].

For more than a century, researchers have developed basic concepts and predicting tools to facilitate the selection of the most effective surfactant for a given application. This started in the 1910's with the Bancroft's rule which stated that the stirring of a Surfactant/Oil/Water (SOW) mixture tends to provide the emulsion whose external phase contains most of the surfactant [2,3]. After World War II, many synthetic nonionic surfactants were marketed including a wide range of polyethoxylated (PEO) fatty alcohols, alkyl phenols and sorbitan esters. In the same period, Griffin introduced the well-known Hydrophilic-Lipophilic-Balance (HLB) to approximately quantify the relative affinity of PEO nonionic surfactants for water and oil [4,5]. Despite its inaccuracy, the HLB scale is still widely used in industry because of its extreme simplicity. Actually, it is based on an empirical equation, unsuitable for non-ethoxylated surfactants and which does not take into account the effect of some essential variables such as temperature [6]. Afterwards, several other more precise concepts with fundamental and experimental aspects emerged. In 1954, Winsor introduced a theoretical concept to characterize SOW systems, namely the ratio $R = A_{co}/A_{cw}$, where A_{co} and A_{cw} reflect the relative interaction energies between the surfactant adsorbed at the interface and the aqueous and oil phases respectively [7,8]. When the interactions of the surfactant with oil and water are equal, i.e. when $R = 1$, the formulation of the SOW system is said to be "optimum" because the interfacial tension γ_{ow} between the oil and water phases exhibits a more or less pronounced minimum. Furthermore, when γ_{ow} is ultra-low (typically $< 10^{-2}$ mN/m) and the interfacial film very flexible [9], a three-phase system (Oil/Microemulsion/Water), named Winsor III and noted WIII, spontaneously forms for thermodynamic reasons [10]. This minimum γ_{ow} at optimum formulation of equilibrated SOW systems was found to correspond to other phenomenological events for the same emulsified

systems (Fig. 1), namely the phase inversion of the emulsion [11] and a minimum emulsion stability [12] and viscosity [13].
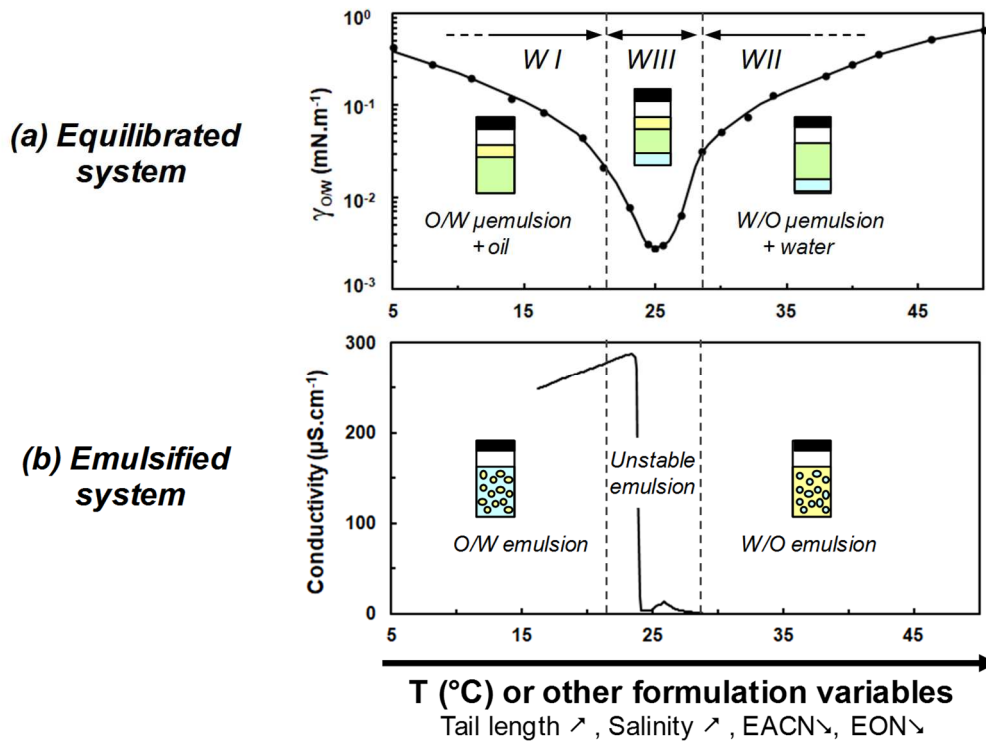

Figure 1. Characteristic phenomena occurring at the "optimum formulation" of the $C_{10}E_4$/n-Octane/Water system at different temperatures (a) Equilibrated system: deep minimum of W/O interfacial tension and three-phase system with a middle microemulsion phase containing the same amount of oil and water and (b) Emulsified system: obtention of O/W, unstable, or W/O emulsion depending on whether the system is emulsified before, at, or after the optimum temperature and phase inversion of the stirred system detected by a sudden drop of conductivity. Data from [14,15].

Winsor's R ratio is conceptually appealing because it takes into account most effects acting on the surfactant molecules located at the interface, but it is however limited by the fact that interaction energies cannot be experimentally determined. In 1964, Shinoda proposed an effective experimental method to identify the "optimum formulation" of PEO-surfactant/Oil/Water systems. It is based on the determination of the so-called "Phase Inversion Temperature" (PIT) of stirred SOW systems from O/W to W/O emulsion detected by visual observation or steep drop in conductivity (Fig. 1) [16]. The emulsion inversion results from the strong variation of the hydrophilicity of the PEO chain of nonionic surfactants when changing temperature. It was an innovative approach to probe SOW systems using a continuous scan of the temperature variable to accurately determine a characteristic event.

In the second half of the 1970's the ten-times increase in petroleum price resulted in an extensive R&D campaign dedicated to the attainment of ultralow tension γ_{ow} which is a prerequisite for an effective chemical Enhanced Oil Recovery (EOR). Consequently, the studies were essentially focused on crude oils or their main components (hydrocarbons) and cheap anionic commercial surfactants such as alkyl benzene sulfonate. Furthermore, the tested variables were the important ones to formulate the injected slug, i.e. the brine salinity, the oil nature and the composition of the surfactant/co-surfactant mixtures, with less interest for the temperature since it has only a weak influence on the hydrophilicity of ionic surfactants and because, in real cases, this parameter is imposed by the reservoir conditions.

In the 80's, empirical correlations for the attainment of the optimum formulation [17] led Salager to develop the "Hydrophilic-Lipophilic-Deviation" (HLD) as a dimensionless linear relationship including all the formulation variables [18]. HLD turned out to be an effective tool to formulate micro- and macro- emulsions with predefined morphologies [19,20] because it allows to calculate trade-off effects between variables on a numerical basis and to determine how to enhance solubilisation [21,22]. Later, it was shown that the optimum formulation occurring when HLD = 0, also corresponds to other specific values of theoretical descriptors of the interfacial film, i.e. a spontaneous mean curvature equal to 0 and an effective packing parameter equal to 1 [23]. In the HLD equation, the hydrophobicity of *n*-alkanes is simply expressed by the Alkane Carbon Number (ACN) whereas for other oils Cash *et al.* introduced the notion of Equivalent Alkane Carbon Number (EACN) which corresponds to the *n*-alkane exhibiting a hydrophobicity equivalent to that of the oil under study [24,25]. However, most EACN values of oils were determined by studying pseudo-ternary SOW systems containing either technical nonionic surfactants [26,27] or anionic surfactants in the presence of additives such as salt and medium chain alcohols [25] which may lead to different values of reported EACNs because of partitioning effects [28]. For instance, Szekeres et al. found an EACN value of $\approx$ 6 for limonene with a salinity scan of the sodium dihexyl sulfosuccinate/limonene/water system [29] whereas our group found a significantly lower value ($\approx$ 2) with a temperature scan of the C_8E_4/limonene/water system [30].

In order to determine unquestionable values of EACN of pure oils, Queste *et al.* developed the Fish-Tail-Method (FTM) based on the "fish diagrams" of true ternary systems C_iE_j/Oil/Water [31]. These diagrams are built by determining the boundaries between the mono-, di- and tri-phasic zones of a C_iE_j/Oil/Water system as a function of temperature and percentage of surfactant while maintaining the Water-to-Oil Ratio (WOR) equal to one. The

most characteristic point of such a diagram is the so-called "fish-tail-point" localized at the temperature T* and the surfactant concentration C* where the body and the tail of the fish meet (Fig. 2c and 3). With *n*-alkanes as references, consistent values of EACN of alkylbenzenes, alkylcyclohexanes, squalene, dibutyl ether and isopropyl myristate could thus be determined. The advantage of this method is the use of simple SOW systems, consisting of only three well-defined components, in particular a pure C_iE_j surfactant avoiding thus the partitioning complex issues and, providing reproducible and unambiguous EACN values regardless the surfactant concentration. Since then, series of oils including triacylglycerols, terpenes, esters and polar fragrance molecules have been investigated with the same method [30,32–34]. More recently, the EACN values of non-polar and polar oils have been successfully rationalized from their molecular structures using the COSMO-RS theory based on quantum mechanics and statistical thermodynamics [35,36].

This review describes in detail the Fish-Tail-Method (FTM) for determining accurately the EACN of oils with well-defined structures, the PACN (Preferred Alkane Carbon Number) of pure C_iE_j surfactants as well as their temperature sensitivity parameter τ. A simplified expression of the HLD equation including only those 3 meaningful parameters is used. Taking as reference the fish-tail-temperatures of the *n*-alkanes, the PACNs of 17 C_iE_j amphiphiles and the EACNs of 125 pure oils are determined from the fish-tail-temperatures T* of true ternary C_iE_j/Oil/Water systems reported in the literature. The PACNs are compared with other descriptors of amphiphilicity, namely, the cloud point, the HLB number and the PIT-slope value. Then, the apparent EACN of mixed oils is discussed on the basis of the difference in oils polarity. Finally, the physical chemistry underlying the EACN concept is explained with the Effective-Packing-Parameter [37,38] and modelled with the COSMO-RS theory .

2   Emergence of the HLD equation

2.1   Single variable scan to detect the optimum formulation

As mentioned above, the optimum formulation can be detected through the PIT for thermo-sensitive PEO-surfactant/O/W systems (Fig. 1). The PIT method provides an accurate measurement of the respective effects of all formulation variables including the nature of ingredients (surfactant, co-surfactant, oil, electrolytes, additives), as well as temperature and pressure [39] In addition, it is widely used in industry to prepare finely disperse and stable O/W emulsions [40]. Though PIT is limited to thermo-sensitive surfactants, this method is a precursor of the further developments for the detection of the optimum formulations through a

sharp experimental event. However, its main drawback is the frequent use of technical-grade surfactants consisting of complex mixtures of oligomers which differently fractionate between the oil and water phases [41,42]. As a consequence, the measured PIT, which is governed by the actual composition of surfactants at the interface, considerably varies with the surfactant concentration [16] and the WOR [43,44] and thus result in uncertainties for both ionics and nonionics. Fortunately this issue can be avoided by resorting to pure though costly PEO-surfactants commercially available at the lab scale.

In a completely different context, the attainment of the ultra-low interfacial tension required for EOR led the researchers to develop the so-called monodimensional formulation scan technique based on the monitoring of the phase behaviour when continuously changing a single formulation variable while maintaining all others constant [45]. The scanned formulation variable was either a characteristic of the oil reservoir (oil type, water salinity or temperature) or a variable specific of the injected aqueous fluid (salinity, nature and concentration of surfactant, alcohol). The optimum formulation was identified either through the detection of a deep minimum of γ_{ow} or by the formation of a middle-phase microemulsion containing equal amounts of water and oil. In the first EOR studies the scanned variable was the oil nature which may be mimicked by liquid n-alkanes of ACNs varying from 5 to 16 [24,25]. Then, with anionic surfactants, it was the salinity in log scale, or the tail length with the same polar head (sulfate, sulfonate or carboxylate) [46]. For PEO-surfactants the scanned variable was the average ethoxylation EON [43,47] with the same tail group or the temperature which has a strong effect on their hydrophilicity [39].

2.2   Generalized multivariable HLD relationship for multidimensional scans

One single variable scan provides only limited information since it corresponds to a specific value of all other variables. To overcome this issue, Salager developed a method changing two variables at the same time around the optimum formulation, through a so-called "two-dimensional scan", which results in a compensation effect. One variable y is set to different discrete values while the other one x, preferentially a variable which exhibits a strong effect, is changed continuously in order to restore the optimum formulation. This procedure, applied to all influential variables, allows determining in which direction and how strongly each variable modifies the affinity of the interfacial film for the aqueous or oil phase respectively. Most of the two-dimensional graphs plotting the values of x and y corresponding to optimum formulations (with all other variables constant) were found to be approximately linear.

These findings led Salager to propose a phenomenological linear relationship called HLD including all formulation variables and expressing quantitatively the deviation of a given SOW system from the optimum formulation. In a first step, he built up such an equation for anionic surfactants as they were the major surfactants used for EOR [17]. Then a similar equation (1) was developed for the PEO surfactants such as the ubiquitous ethoxylated alcohols (C_iE_j), of interest here [47].

$$HLD = (\alpha - EON) - k.EACN + b.S + f(A) + c_T(T - 25) \qquad (1)$$

Where

- α expresses the hydrophobicity of the surfactant tail. It increases almost linearly with the number of carbon atoms in the alkyl chain.

- EON is the exact or average number of ethoxy units in the hydrophilic head.

- $EACN$ is the Equivalent Alkane Carbon Number. It is a characteristic of the oil which increases with its hydrophobicity. It is equal to ACN when the oil is an n-alkanes. k is a numerical coefficient that depends on the sensitivity of the surfactant to variations in ACN.

- S is the salinity of the aqueous phase in wt. % of salt. b is a numerical coefficient that depends on both the nature of the salt and the surfactant sensitivity to variations in salinity.

- A is the weight percent of alcohol A optionally added as a co-surfactant to increase the flexibility of the interfacial film and its affinity for the oil phase. $f(A)$ is a function depending on the nature and the concentration of the alcohol A.

- T is the temperature in °C and c_T is a numerical coefficient expressing the sensitivity of the surfactant to temperature variations.

When HLD = 0, the formulation of a SOW system is called "optimum" since the interfacial film has the same affinity for water and oil and affords a maximal co-solubilisation of them with a minimum amount of surfactant. Although empirical, the relationship (1) allows to predict the experimental conditions required to obtain an optimum formulation for a given system SOW knowing the values of the various parameters. By analyzing the numerous results describing optimum formulations in the literature, Salager *et al.* have estimated the characteristic coefficients for the most common surfactants, salts and co-surfactants [19,46]. Consider, for example, the ternary system $C_{10}E_4$/n-Octane/Water that is often used as a reference SOW system for measuring the EACN of oils [31] and the true HLB of surfactants by the PIT-slope method [48,49]. For this system, $\alpha = 5.3$, $EON = 4$, $k = 0.15$, $EACN = 8$,

$c_T = 0.06$ [19] and, since it is free of salt and alcohol, S and A are both zero. Accordingly, when the formulation is optimum ($HLD = 0$), equation (1) simplifies to (2) and the calculated optimum temperature T* is 23.3 °C, close to the experimental value 24.3 °C [50].

$$0 = (5.3 - 4) - 0.15x8 + 0 + 0 + 0.06x(T^* - 25) \qquad (2)$$

In practical terms, the optimum formulation is an important reference point for the formulator because it corresponds to the conditions for which the microemulsion middle-phase co-solubilises the maximum amount of water and oil. On the other hand, when HLD is not equal to zero, the HLD value represents the deviation of a given formulation from the optimum condition. Knowledge of this value can help to find suitable experimental conditions for obtaining fine and stable emulsions for a given emulsification method. Indeed, the finest O/W and W/O emulsions are approximately located at one HLD unit on either sides of the optimum formulation (Fig. 1b). It should be noted that the exact position of fine emulsions depends on the formulation of the SOW system but also on the WOR and the emulsification process [11,51,52].

3   Normalized and simplified HLD equation for nonionic surfactants

Thanks to its versatility and effectiveness, the HLD equation (1) is often used in the oil industry for finding the optimum formulation in EOR applications [53–56]. However, it is less frequently used in other applications because of its apparent complexity. Actually, the overall Eq. 1 includes 10 variables, 6 of them *(α, EON, EACN, S, A, T)* are required to define the SOW systems, plus 3 characteristic coefficients *(k, b, c_T)* and one function, $f(A)$, which express the sensitivity of the surfactant towards the different variables. As a consequence, when formulators have to select a suitable surfactant for a particular application, they often resort to the poorly reliable but much simpler HLB scale.

Since the objective of this review is to determine as accurately as possible the hydrophobicity of oils and the amphiphilicity of nonionic surfactants, we chose to consider the phase behaviour of the simplest possible SOW systems but nevertheless allowing a continuous variation of the HLD in a wide range. To simplify the current HLD equation (1) we kept the variables essential for characterizing a true ternary SOW system and we deleted other non-essential variables. Three variables are unavoidable (i) $(\alpha - EON)$ which expresses the amphiphilicity of the surfactant at 25°C without salt and co-surfactant, (ii) $EACN$ which represents the hydrophobicity of the oil and (iii) $c_T(T - 25)$ which reflects the influence of temperature on the amphiphilicity of the surfactant. Conversely, the two other terms $b.S$ and $f(A)$ are not strictly necessary for our SOW systems and may be discarded. Accordingly, for

nonionic SOW systems free of salt and co-surfactant, equation (1) is simplified to equation (3).

$$HLD = (\alpha - EON) - k.EACN + c_T(T - 25) \qquad (3)$$

Relation (3) still suffers from three major issues that need to be corrected. First, the numerical value of HLD that expresses the system deviation from the optimum formulation does not have a straightforward physical meaning. Second, the term $(\alpha - EON)$ incorrectly implies that the hydrophilicity of a PEO surfactant is strictly proportional to the number of ethoxy units. Third, equation (3) has a useless parameter since only the optimum formulation (HLD = 0) has a clear physicochemical definition (minimum W/O interfacial tension). Therefore, the expression (3) can be divided by any coefficient and still be equal to zero at the optimum formulation. In general, the coefficient in front of the scanned variable is arbitrarily taken as unity. For nonionic ethoxylated surfactants, the usual scan is the surfactant hydrophilicity, as its ethoxylation number EON and thus the coefficient in front of EON is taken as unity (Eq. 3). Alternatively, the temperature [57] or the number of carbons of homologous hydrocarbon oils [47] can be employed as scan variables. Here, we prefer to choose EACN as the scanning variable because this parameter is common to all SOW systems based on ionic or nonionic surfactants. In addition, dividing the equation (3) by k highlights PACN as the simplest and the most relevant parameter to characterize surfactant amphiphilicity. With this convention, the deviation from the optimal formulation is expressed in ACN units. Such a scale is unambiguous since, by definition, the ACN of an n-alkane oil is equal to its number of carbons independently of the surfactant type which allows straightforward comparisons of PACNs as stated in our first review [19].

In light of all these considerations, *a "normalized" version of the HLD equation, noted HLD$_N$ (Eq. 4), is proposed for all SOW systems* [58]. This new way of writing the HLD equation has already been published with the index "u" instead of "N" to indicate that the equation is "unique" for all types of surfactants [59,60]. It must be noted that, for more complex SOW systems involving salts and/or co-surfactants, the additional terms b.S/k and f(A)/k should be added to the equation (4).

$$HLD_N = PACN - EACN + \tau(T - 25) \qquad (4)$$

Where,

- $PACN = [\alpha - EON]/k$ expresses the amphiphilicity (i.e. the "true" HLB) of the surfactant at 25°C through its "Preferred *ACN*", whose meaning is explained in details in the next paragraph.

- *EACN* expresses the hydrophobicity of the oil. It is equal to the number of carbon atoms (ACN) when the oil is an n-alkane.

- $\tau = c_T/k$ reflects the sensitivity of the surfactant towards temperature.

Equation (4) assumes that, for a SOW system at the optimum formulation ($HLD_N = 0$), the so-called "optimum temperature", denoted T*, varies linearly with *ACN* as reported in the literature for numerous C_iE_j/n-Alkane/Water systems [50,61].

Writing the HLD_N in the simplified form (4) has also the advantage of giving a understandable physical meaning to the *PACN* of a surfactant and to the deviation HLD_N of a given formulation from the "optimum" conditions [46]. *Thus, the "Preferred Alkane Carbon Number" (PACN) of a surfactant corresponds to the number of carbon atoms of the n-alkane (or a mixture of n-alkanes) which gives an optimum formulation at 25 °C in the absence of salt and co-surfactant.* For instance, the PACN of $C_{10}E_4$ is equal to 8.1 because the system $C_{10}E_4$/n-Octane/Water spontaneously forms an optimum formulation close to 25 °C with a strong minimum of the interfacial tension between the oil and the water excess phases (Fig. 1a) [14]. Moreover equation (4) shows that, for non-optimum C_iE_j/n-Alkane/Water systems ($HLD_N \neq 0$), a decrease of one HLD_N unit corresponds to a physicochemical modification similar to that provided by adding one additional CH_2 unit to the *n*-alkane oil. It is worth to be noted that the concept of PACN was introduced 40 years ago by Salager for anionic surfactants under the very explicit but terrific acronym EPACNUS meaning "Extrapolated Preferred Alkane Carbon Number at Unit Salinity without alcohol" [17] and by Wade *et al.* under the name N_{min} to indicate that it is the carbon number of the n-alkane leading to a minimum interfacial tension [41]. The thermal sensitivity parameter of the surfactant τ is expressed in °C^{-1}. Its numerical value corresponds to the change of HLD_N induced by a temperature increase of 1°C.

4   Fish-diagrams of C_iE_j/n-Alkane/Water systems

4.1   Fish-cut in the phase prism C_iE_j/n-Alkane/Water-Temperature

Nowadays, oligomeric mixtures of PEO alkyl ethers (C_iE_j) are, by far, the most industrially used nonionic surfactants because of the simplicity of their synthesis and the versatility of their properties. Indeed, the length i of the hydrophobic chain and the average number of ethoxy units j can be easily tuned to fit the amphiphilicity of C_iE_j for obtaining the desired functional properties. The shortest compounds such as C_4E_1 and C_6E_2 belong to a particular family of hydrotropes known as solvo-surfactants as they combine some solvent

characteristics (volatility, low viscosity, no lyotropic liquid crystals) as well as typical surfactant properties (interfacial activity, aqueous solubiliser). Technical grade C_iE_j with long chains (C_{16}-C_{18}) are mostly used for their emulsifying properties, while those with intermediate chains (C_8-C_{14}) are the most widespread because they belong to the surfactant cocktail present in detergents and cosmetics [62]. The physicochemical properties of well-defined C_iE_j have also been extensively studied because they are commercially available in the pure state for a wide variety of i and j values. Moreover, as the hydrophilicity of PEO segments is strongly thermo-sensitive, the temperature is a very convenient variable to continuously and reversibly tune the effective amphiphilicity of C_iE_j surfactants in order to find the optimum formulation. The phase behaviour of C_iE_j/n-Alkane/Water-Temperature systems can be represented in a prism formed by the superimposition of a series of Gibbs diagrams at various temperatures (Fig. 2).

Gibbs diagram   Shinoda cut   Fish-cut
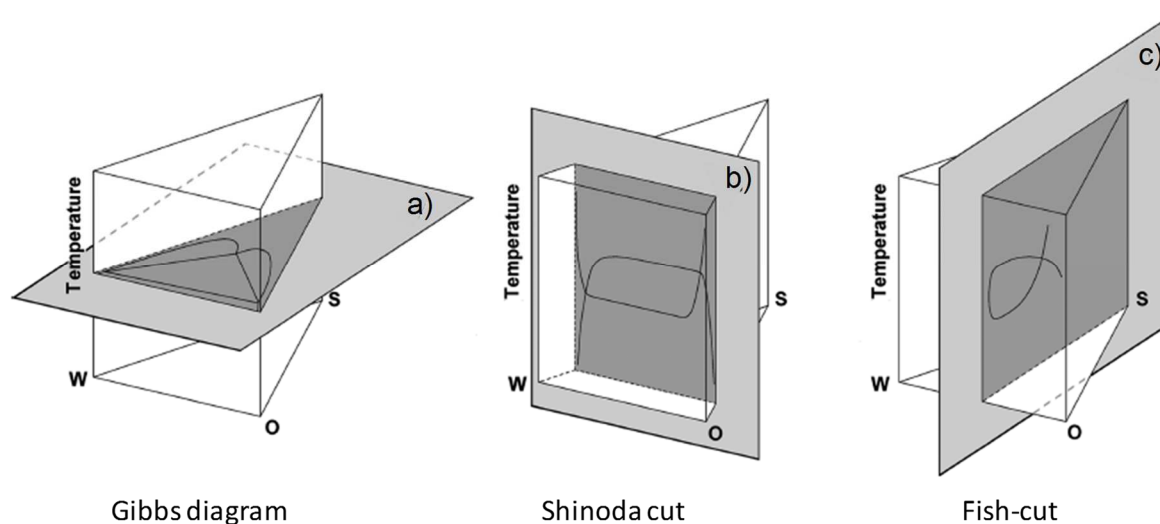
Figure 2. Two-dimensional planar cuts of a C_iE_j/Oil/Water-Temperature prism at constant (a) temperature (Gibbs diagram), (b) surfactant concentration (Shinoda-cut), or (c) WOR (Fish-cut) [63]

Experimental exploration of the entire prism is however time-consuming and not necessary to highlight the influence of temperature and compositional variables on the phase behaviour. That is why such systems are usually studied by making planar cuts through the prism. For instance, Gibbs diagrams and the so-called "Shinoda-cuts" [64,65] are respectively the 2D diagrams obtained by maintaining the temperature or the weight percentage of surfactant at constant values (Fig. 2a and 2b). Regarding the fish-cut which is of special interest here, the WOR is kept equal to 1, while the variables are the temperature and the wt% of C_iE_j surfactant in the mixture [66,67] (Fig. 2c). As an example, the fish-cuts of the C_8E_4/Oil/Water systems for different oils are shown in figure 3.

Figure 3. Fish-cuts through the phase prism C_8E_4/Oil/Water-Temperature with WOR = 1. The fish-tail point (X) is characterized by the concentration C^* and the optimum temperature T^* whereas the wt. % of surfactant at the fish-head is equal to C_0. The width of the three-phase body is between T_{low} and T_{up}. Fishes corresponding to cyclohexane, hexane and tetradecane are redrawn from [61,68].

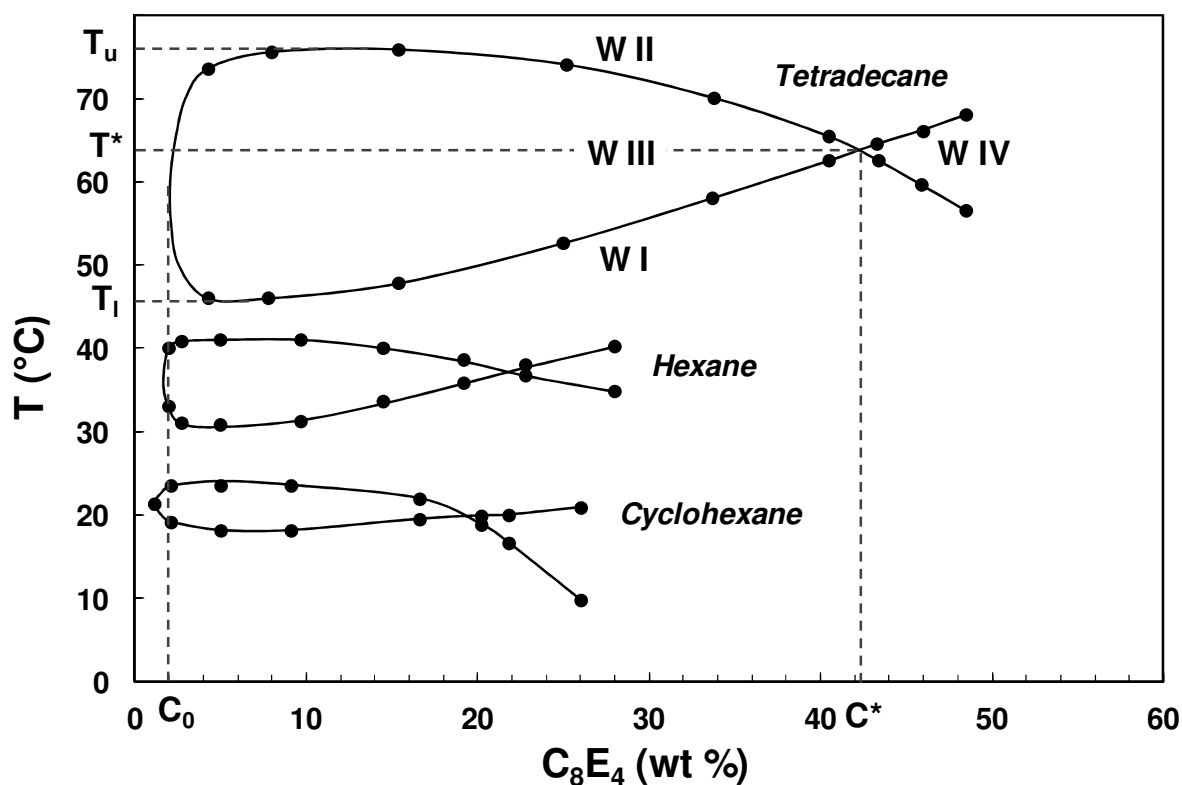The section through the three-phase body has the shape of a fish whose body contains the three-phase region (WIII), the tail the one-phase region (WIV) and the exterior of the fish, the two-phase regions (WI and II). The optimum temperature T^* of C_iE_j/*n*-Alkane/Water systems can be detected by different methods, namely the minimum W/O interfacial tension [14] the middle of the three-phase zone ($T^* = [T_{low}+T_{up}]/2$) [61] the phase inversion temperature (PIT) of the pre-emulsified SOW mixture [16]. However, these measurements are either fastidious (interfacial tension) or ambiguous (middle of the three-phase body and PIT) because T^* could vary with the surfactant concentration and WOR. Therefore, we preferred to consider the fish-tail-temperature T^* of the so-called X point, localized between the body and the tail of the fish, because it is unambiguous, easily determined and many reliable values are available in the literature. Indeed, the X point is very important both for practical and theoretical reasons. On the one hand, this point corresponds to the highest mutual solubility between oil and water with the minimum amount of surfactant. On the other hand, this X point is the pivot point for a reliable characterization of C_iE_j/Oil/Water systems since its ordinate T^* on the temperature

scale unambiguously expresses the hydrophobicity of the oil whereas its abscissa C* on the surfactant scale is a measure of the performance of the amphiphile. Many fish diagrams have been established with high accuracy for various C_iE_j and a large series of *n*-alkanes, the most reliable of them are reported in Tables 1 and 2. It is worth noting that the fish-tail-temperatures T* reported by Kahlweit and Strey groups for the C_8E_4 and $C_{10}E_4$/*n*-Alkanes/Water systems [50,61] are somewhat lower than the values reported by our group [30,31]. This discrepancy can be explained in part by the differences in experimental protocols used to build fish diagrams (i.e. wt.% *versus* vol.%). For example, for the $C_{10}E_4$/*n*-octane/water system with a WOR (w/w) equal to one, Pizzino *et al.* measured a T* value of 25.7 °C whereas the same system with equal volumes of oil and water provides an X point slightly shifted downward with T* = 24.8 °C [63] More importantly, traces of impurities into the commercial "pure" C_iE_j surfactants arising, either from the starting materials (C_iOH and E_j), or from oxidative degradation products [69] can significantly alter the fish-tail temperature. For instance, a deliberate addition of 0.3 wt % of *n*-octanol and E_4 in the C_8E_4/*n*-Octane/Water system was found to decrease the fish-tail-temperature by 5 °C. Furthermore, it was found that commercially available C_8E_4 (e.g. from Fluka) often used to build fish diagrams has a much lower CP (37.4 °C) than the one of freshly synthesized and distilled sample (40.8 °C) [31] in agreement with the value reported by Schubert *et al.* for a highly purified sample of C_8E_4 (40.8 °C) [70,71]. Therefore, it is recommended to always use the same method and the same sample of C_iE_j for establishing the calibration line with the *n*-alkanes and for measuring the T* of the oil under study.

Table 1. Selected values of fish-tail-temperatures T*(°C) for a series of C_iE_j/*n*-Alkane/Water systems. Preferred Alkane Carbon Numbers PACN (in ACN units) and temperature sensitivity coefficients τ (in ACN/°C units). HLB values calculated according to Griffin's equation $HLB = 20\,MW_{E_j}/MW_{C_iE_j}$ and PIT-slope values, dPIT/dx [49,60].

C_iE_j		T* for n-alkanes of various ACN							PACN	τ	HLB	$\dfrac{dPIT}{dx}$	Ref
i	j	6	7	8	10	12	14	16					
4	1	-0.8	-	16.8	33.9	51.2	68.6	-	9.0±0.2	0.12	10.3	-	[73]
4	2	63.1	-	79.6	95.0	-	-	-	1.2±0.4	0.13	13.0	-	[73]
6	2	-	-	7.4	18.4	27.5	-	40.9	11.9±0.2	0.24	11.1	-	[50,74]
6	3	36.0	-	44.2	52.8	60.9	68.9	-	3.3±0.4	0.24	12.7	-	[50,73]
6	4	65.8	71.4	77.5	-	-	-	-	-1.5±1.0	0.18	13.9	-	[30]
8	3	9.2	12.0	15.9	22.1	28.0	33.7	38.6	11.2±0.2	0.34	11.4	-	[50,61,75]

…

i	j								PACN	τ	HLB		Ref
8	4	37.4	43,8	46.1	54.5	63.9	71.3	77.9	2.7±0.4	0.25	12.6	-	[30]
8	4	34.5	-	41.7	48.0	54.6	61.0	68.1	3.0±0.4	0.30	12.6	-	[50,61]
8	5	54.4	-	61.0	68.3	75.5	82.7	-	-2.4±1.0	0.28	13.5	34	[61]
8	6	-	-	75.8	83.8	-	-	-	-6.3±2.0	0.28	14.3	-	[61]
10	4	19.5	-	25.0	30.5	35.5	41.5	47.0	8.1±0.2	0.36	11.6	0	[31]
10	4	-	-	24.3	30.1	35.4	40.2	-	8.0±0.2	0.38	11.6	0	[50]
10	5	39.5	-	45.1	50.0	55.5	63.5	-	1.3±0.4	0.34	12.5	22	[50,76]
10	6	-	-	61.4	-	-	-	-	-4.1±2.0	0.33	13.3	-	[50]
12	4	7.5	10.0	12.8	19.9	-	31.6	-	11.8±0.2	0.33	10.7	-9.2	[50,73]
12	5	-	28.4	32.6	38.5	43.8	48.7	54.0	5.4±0.4	0.36	11.7	6.8	[50,61,77]
12	6	43.0	-	48.7	55.5	-	65.2	71.5	-0.5±1.0	0.36	12.5	33	[50,75]
12	7	55.0	-	62.6	68.0	-	-	83.1	-4.7±2.0	0.35	13.2	63	[50,73]
12	8	-	71.0	-	78.0	-	-	93.0	-9.5±3.0	0.35	13.7	98	[78]
14	6	-	-	-	-	50.6	-	-	-	-	11.8	-	[79]

Table 2. Fish-tail-temperatures T*(°C) for C_iE_j/long-chain n-Alkane/Water systems where the n-alkane oils are solid at room temperature. The symbol C_k corresponds to an n-alkane with k carbons.

C_iE_j		T* for n-alkanes of various ACN								PACN	τ	HLB	Ref
i	j	18	20	22	24	26	28	30	32				
10	4	54.0	59.0	-	71.0	-	79.0	-	-	8.1±0.2	0.36	11.6	[31]
12	5	56.2	60.2	-	-	-	-	-	-	5.4±0.4	0.36	11.7	[80]
14	6	-	66.3	69.4	72.8	74.9	78.3	-	-	a	0.67	11.8	[80]
16	6	-	-	-	-	-	66.7	68.9	70.9	a	0.95	11.1	[80]

(a) Experimental points are too few and too much above 25°C to provide reliable values of PACNs by extrapolation of the straight segment

4.2 Evolution of the fish-tail-temperature T* with the length of n-alkane oils

Equation (4) assumes that, for a surfactant with given PACN and τ, the fish-tail-temperature T* varies linearly with the chain length of the n-alkanes. This linearity has been verified by Kahlweit and co-workers with numerous C_iE_j/n-Alkane/Water systems [61] for a series of n-alkanes ranging from n-hexane to n-hexadecane. Unexpectedly, Queste *et al.* found that this linearity also holds for much longer n-alkanes up to octacosane (C_{28}) for the system $C_{10}E_4$/n-Alkane/Water [31]. Actually, figures 4a-e clearly show that T* varies linearly as a function of the length of the n-alkane for all the amphiphiles reported in Table 1 and 2.
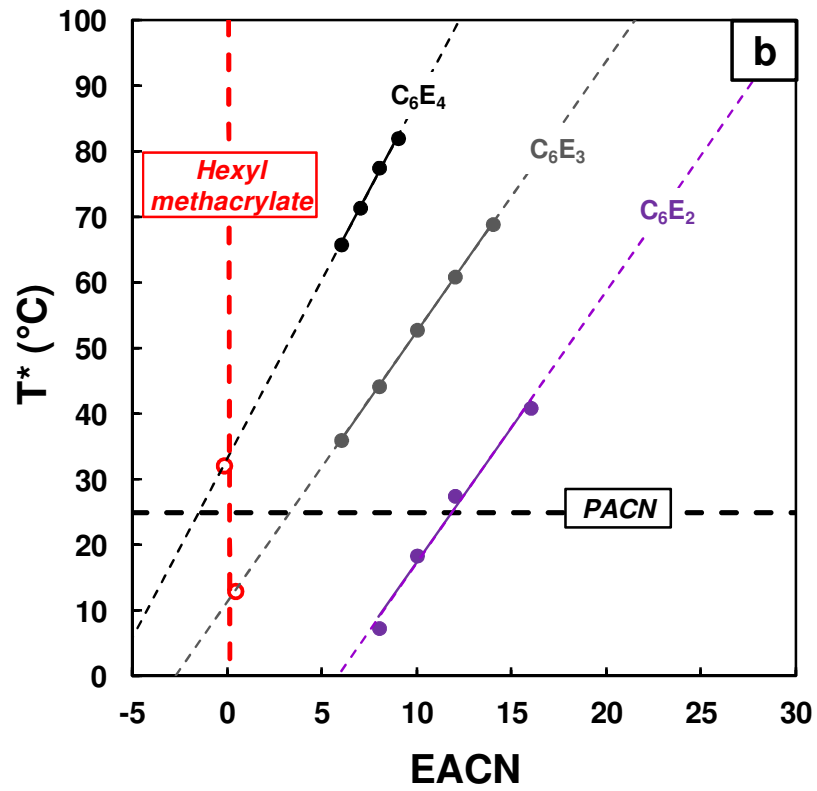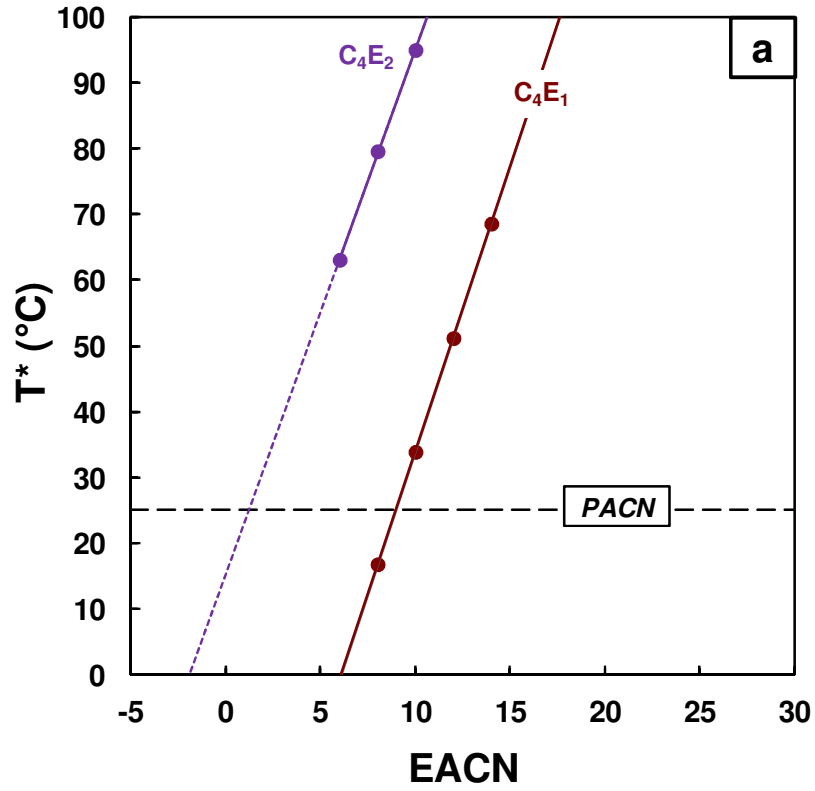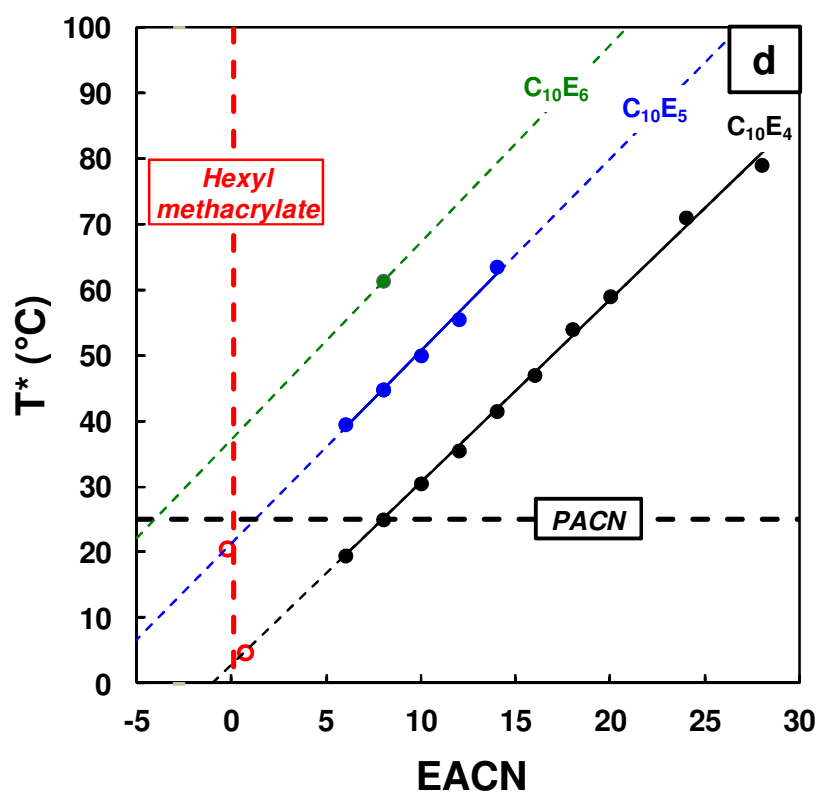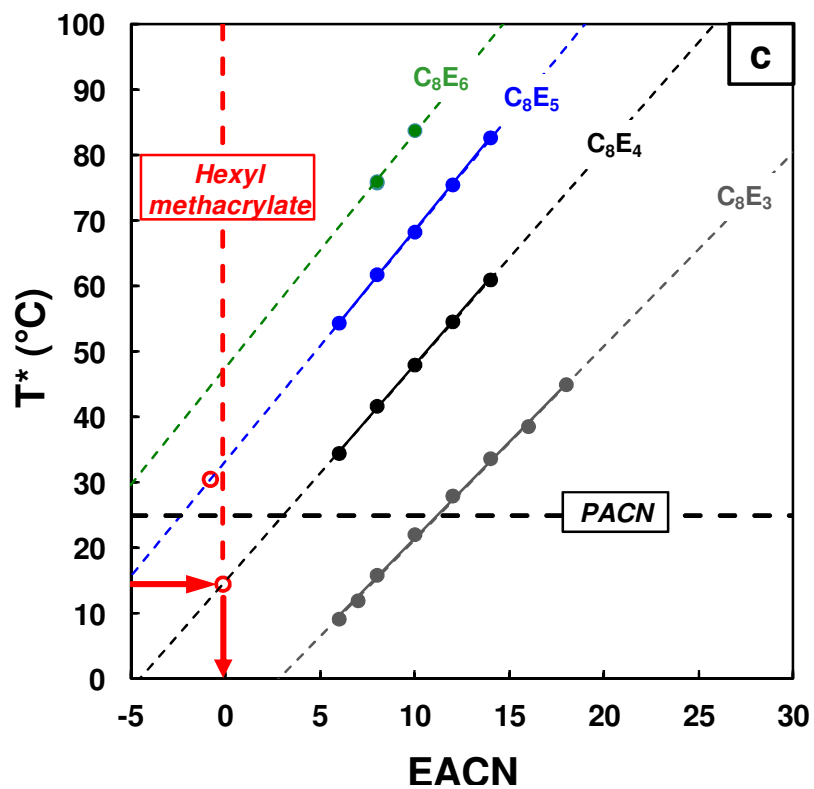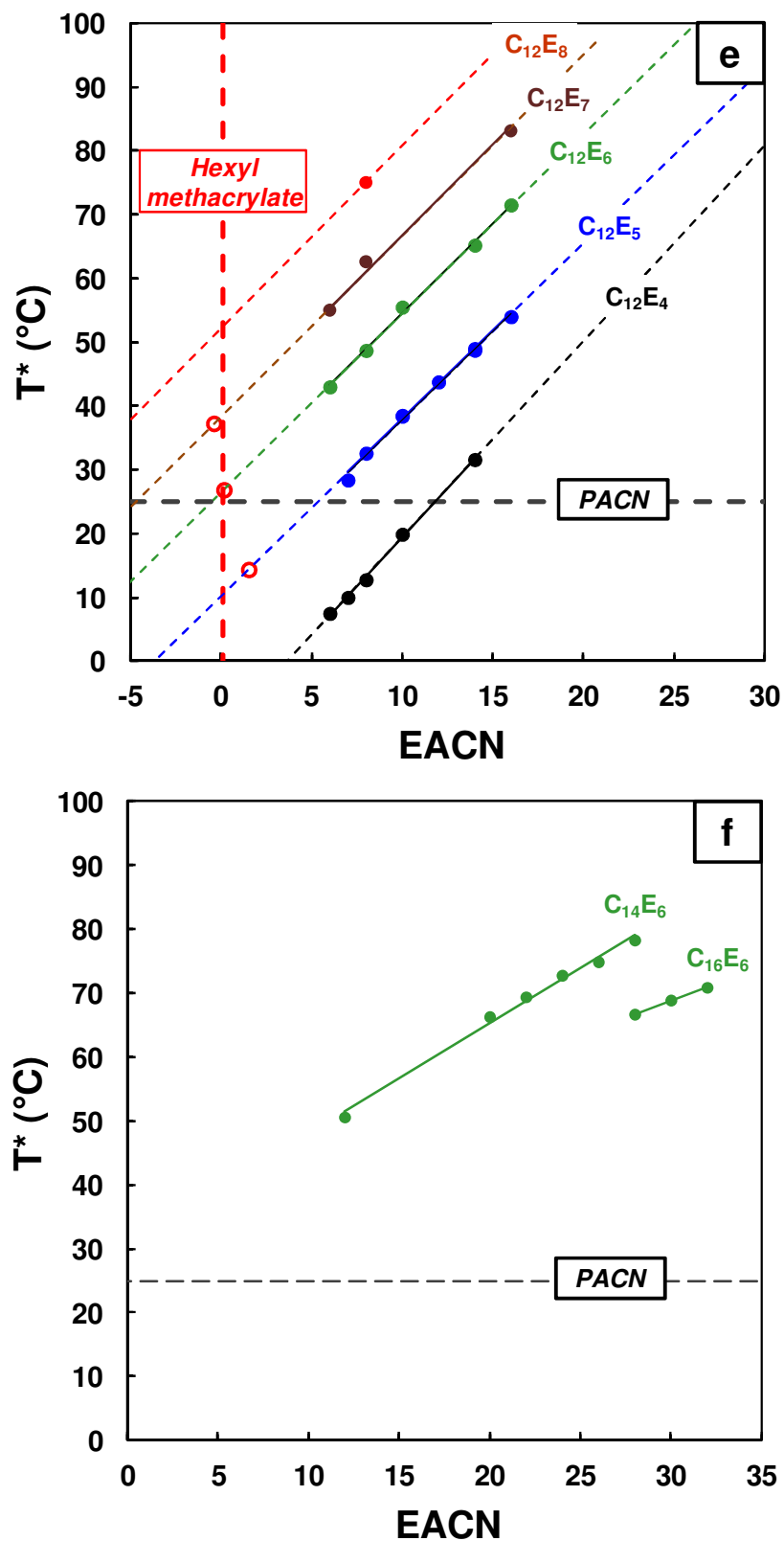
Figure 4. Evolution of the fish-tail-temperatures T* with the length of *n*-alkanes (ACN) for a series of hydrotropes (a) C_4E_j, (b) C_6E_j, and surfactants (c) C_8E_j, (d) $C_{10}E_j$ and (e) $C_{12}E_j$.(f) $C_{14}E_j$ and $C_{16}E_j$ The T* values of hexyl methacrylate (red empty circles) determined by Lade and al. [81] with various C_iE_j are positioned on the extrapolated straight lines corresponding to *n*-alkanes and will be discussed in paragraph 6.

4.3 Evolution of the fish-tail-temperature T* with the number of ethoxy groups

Experimental data summarized in table 1 allow testing the validity of certain underlying assumptions of the original HLD equation (1). According to this equation, the evolution of the fish-tail-temperature T^* of C_iE_j/n-Alkane/H_2O systems free of salt and co-surfactant should be linear as a function of EON if the surfactant tail (C_i) and the n-alkane (ACN) are maintained constant. Actually, figure 5 shows that this is not the case as the addition of further EO groups brings less and less supplementary hydrophilicity to the surfactant. The evolution of T* as a function of EON is not linear but follows approximately a logarithmic law analogous to the empirical relationship found by Gu to express the evolution of the cloud point of C_iE_j surfactants as a function of the logarithm of the number of ethoxy units [82].
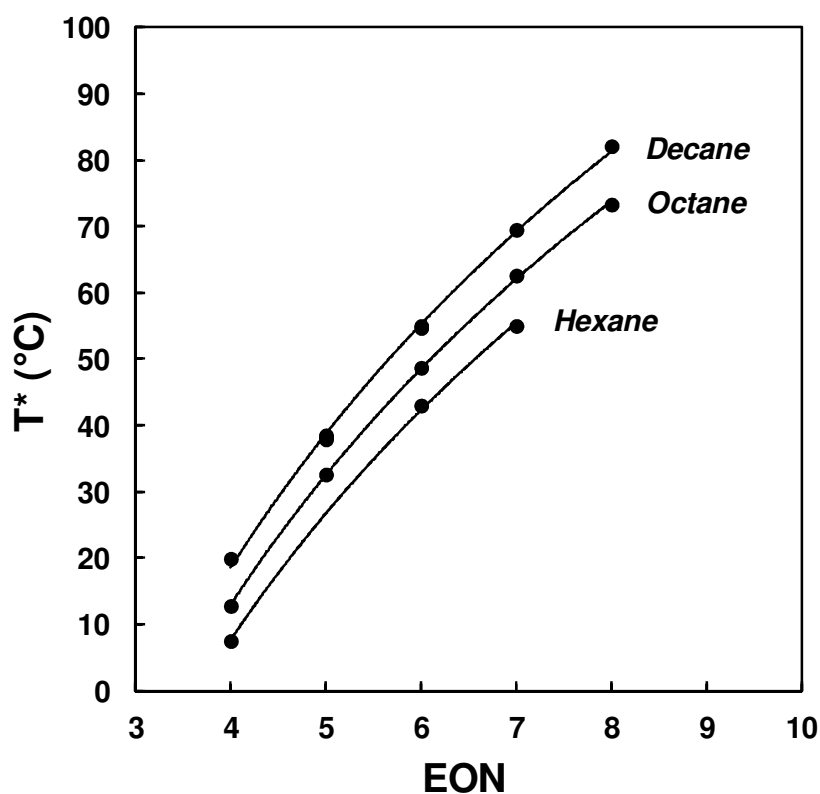
Figure 5. Evolution of the fish-tail-temperature T* for the systems $C_{12}E_j$/n-Alkane/Water with n-hexane, n-octane and n-decane as a function of the number of ethylene oxide groups (EON). The experimental values are fitted with a logarithmic law.

5 Preferred Alkane Carbon Number (PACN) of surfactants

5.1 PACNs and temperature coefficients τ of C_iE_j surfactants

The HLD concept and the associated notion of "optimum formulation" allow classifying surfactants according to their relative lipophilicity and hydrophilicity at 25 °C. This was done

by Salager *et al.* who assessed the coefficients α, k, b and c_T in Eq. 1 for various nonionic ethoxylated surfactants [19,59]. However, these values are not characteristic of the molecular structure but rather approximate because technical-grade surfactants and/or complex SOW systems were used to detect the optimum formulation [18]. A way to ensure the accuracy of PACN values for surfactants in accordance to their specific molecular structure is to consider only true ternary SOW systems based on pure components (surfactants, oils and water) and free of any additive such as salt or co-surfactant. With such systems, T* values are reliable and repeatable, and can be used to compare amphiphiles at 25 °C according to their PACN values. It is noteworthy that the more hydrophilic the surfactant, the lower the PACN contrary to the convention used by Griffin for defining the HLB scale ($HLB = 20\, MW_{EO_j} / MW_{C_iEO_j}$) as shown in Table 1. PACN values for C_iE_j surfactants can be easily determined by locating the intersection of the inclined line corresponding to the C_iE_j under study in figures 4a-e with the horizontal line corresponding to T = 25 °C. For C_4E_1, C_6E_2, C_8E_3, $C_{10}E_4$ and $C_{12}E_4$, the intersections are within the range of liquid *n*-alkanes (C_6-C_{16}) and their PACN values are thus known with good precision ($\pm$ 0.2 unit). On the other hand, other C_iE_j surfactants are more hydrophilic and do not give WIII systems with *n*-alkanes at 25 °C. Therefore, the intersections with the horizontal line are located in the extrapolated part of the straight lines. The more distant it is from the *n*-alkanes zone, the lower its precision because of the uncertainty on the slope of the *n*-alkanes lines. The PACN values for the 19 investigated C_iE_j reported in Tables 1 allow drawing the iso-PACN curves presented in figure 6. Thanks to this abacus, it is possible to graphically predict the PACNs of surfactants of the C_iE_j type including those whose fish-tails are not known (i = 5, 7, 9, 11 and 13).
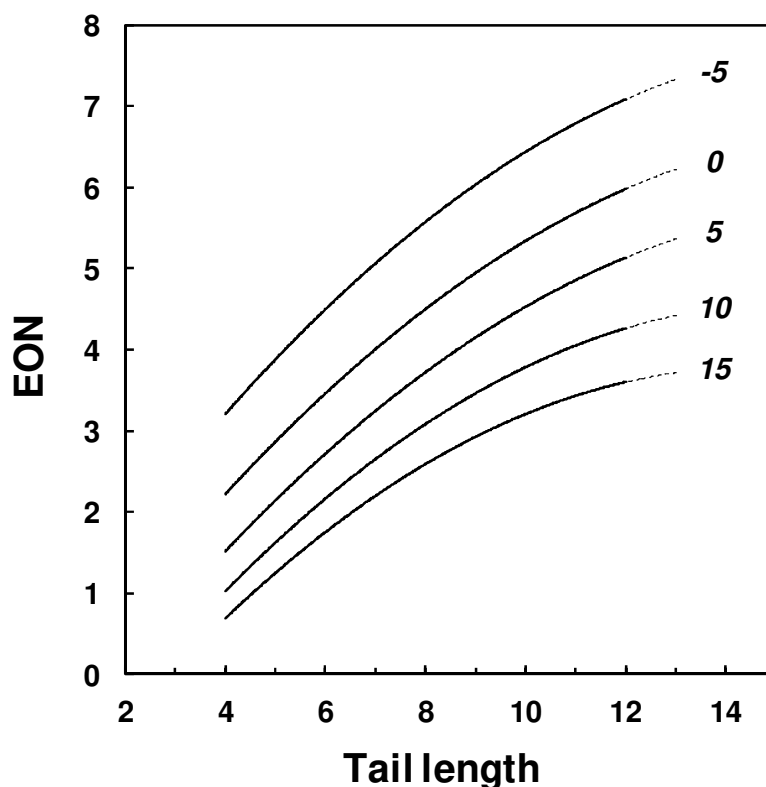
Figure 6. Iso-PACN curves of the C_iE_j amphiphiles as a function of the number of ethoxy groups j and the tail length i. The continuous lines correspond to the experimentally covered domain (i = 4 to 12).

The hydrophilic-lipophilic balance of a surfactant, here called "amphiphilicity" to avoid confusion with Griffin's HLB, is one of the most important characteristics of surfactants. The design of a descriptor capable of quantifying it accurately is part of a long quest that began in 1949 [4]. It is known nowadays that such a descriptor only makes sense insofar as the physicochemical conditions (temperature, pressure, salinity, surfactant concentration, WOR, nature of the oil, additives) are well specified because all these variables of formulation are likely to modify the apparent amphiphilicity of surfactants. Polyethoxylated alcohols being the most widely used and best-studied nonionic surfactants, many descriptors of their amphiphilicity have been proposed. It is therefore interesting to compare their PACNs with the other most commonly used quantitative descriptors, namely, the cloud point CP [83], the Griffin's HLB [5] and the PIT-slope [48,49,60].

5.1.1 PACNs vs Cloud points

In 1964 Shinoda and Arai found that the PITs of pre-emulsified SOW systems were non-linearly correlated with the cloud points (CP) of various technical-grade PEO surfactants [16]. It is well-known that the phase behaviour and the PITs of such SOW systems are driven by

the composition of surfactants localized at the W/O interface which may significantly differ from the composition of surfactants introduced into the medium [84]. Actually, fishes built with technical grade C_iE_j surfactants are twisted upwards leading to inaccuracies and a lack of reproducibility in the value of the PITs [85]. In contrast, PACNs shown in Table 1 are unambiguously determined from the fish-tail-temperatures T* of very pure ($\geq$ 98%) C_iE_j surfactants which do not suffer from the partitioning issues encountered with mixtures of ethoxymers [18]. Accordingly, an even better correlation between PACNs and CPs is expected. Figure 7 shows the evolution of the PACNs of 16 well-defined C_iE_j as a function of the average values of the CPs given in Table 3.

Table 3. Cloud points of C_iE_j surfactants (i = 8, 10 and 12) and hydrotropes (i = 4 and 6) reported in the literature

C_iE_j		Cloud point (°C)				Mean value
1	j					
4	1	44.5[a]	48.7[a]	-	-	46.6
4	2	>100[f]	-	-	-	>100
6	2	0[a]	-	-	-	0.0
6	3	39.6[a]	44.7[a]	45.4[a]	46.0[b]	43.9
6	4	66.1[b]	67.5[a]	-	-	66.8
8	3	8.0[a]	11.0[b]	11.0[f]		10.0
8	4	35.5[a]	39.6[a]	40.3[a]	40.8[b]	39.1
8	5	60.9[a]	61.7[b]	-	-	61.3
8	6	68.0[a]	71.0[a]	74.4[b]	-	71.1
10	4	19.5[c]	20.5[a]	20.5[d]	-	20.2
10	5	40.5[a]	43.6[d]	45.5[a]	-	43.2
10	6	58.0[f]	61.5[a]	62.2[f]	-	60.6
12	4	3.6[a]	6.6[b]	7.0[a]	7.5[a]	6.2
12	5	26.5[a]	30.5[a]	31.5[a]	32.0[b]	30.1
12	6	48.0[a]	50.0[a]	50.4[a]	51.3[b]	49.9
12	7	61.5[d]	65.0[a]	67.2[a]		64.6
12	8	75.3[a]	75.5[a]	79.5[a]	-	76.8

[a] [86], [b] [70], [c] [87], [d] [88], [e] [89], [f] [90]

Figure 7. Correlation between the Preferred Alkane Carbon Number (PACN) of C_iE_j surfactants (black dots) or hydrotropes (red dots) and their cloud points.

An excellent linear correlation ($R^2 = 0.992$) is obtained for the 12 true surfactants (black dots) with C_8, C_{10} or C_{12} hydrophobic tail (Eq. 5).

$$PACN = -0.29 x CP + 14.0 \tag{5}$$

Using the empirical linear relation found by Gu expressing the cloud point as a function of the logarithm of the ethoxy group number j and the length of the tail i [82], the PACNs of the surfactants C_iE_j ($i \geq 8$) can be roughly assessed as a function of i and j according to equation (6)

$$PACN = -64 x \log j + 1.6 x i + 30 \tag{6}$$

However, the red dots corresponding to the hydrotropes with C_4 and C_6 tails are outside the correlation line because these amphiphiles are too short to form well-structured interfacial films at the W/O interface [91]. In addition these hydrotropes do not form micelles and strongly partition both in the oil and the aqueous excess phases and modify their apparent hydrophilicity and lipophilicity [21].

Shinoda and Arai put forward an explanation for the correlation between CPs and PITs based on the hypothesis that "*the cloud point can be regarded as akin to the inversion temperature of an emulsion in which the surfactant plays both the role of emulsifier and oil*". Indeed, it is clear that CPs, PITs and PACNs are mainly governed by the same phenomenon, namely the gradual dehydration of the polyethylene glycol chain of C_iE_j surfactants on increasing temperature which switches progressively the surfactant affinity from water to oil phase.

5.1.2 PACNs vs HLBs

Although obsolete, the HLB number is still often used as a rough guide by formulators who must select suitable surfactants for a given application, such as micellar solubilization, detergency, wetting, O/W or W/O emulsification, foaming, etc... [4]. Indeed, despite its simplicity, the hyperbolic equation used to calculate the HLB of C_iE_j surfactants ($HLB = 20\,MW_{E_j}/MW_{C_iE_j} = 20(44 \times j + 17)/(14 \times i + 44 \times j + 18)$ manages to reflect some important trends of these surfactants. In particular, the non-linear evolution of HLB as a function of j is compatible with the experimental evolution of T* and PACN presented in Figures 5 and 6. Furthermore, it is interesting to compare the HLB values of C_iE_j surfactants with their PACNs in order to see how the two scales match and to determine what range of HLBs can be covered by the fish-tail-method. Figure 8 shows the evolution of the PACNs of 17 well-defined C_iE_j as a function of the HLB number given in Table 1.
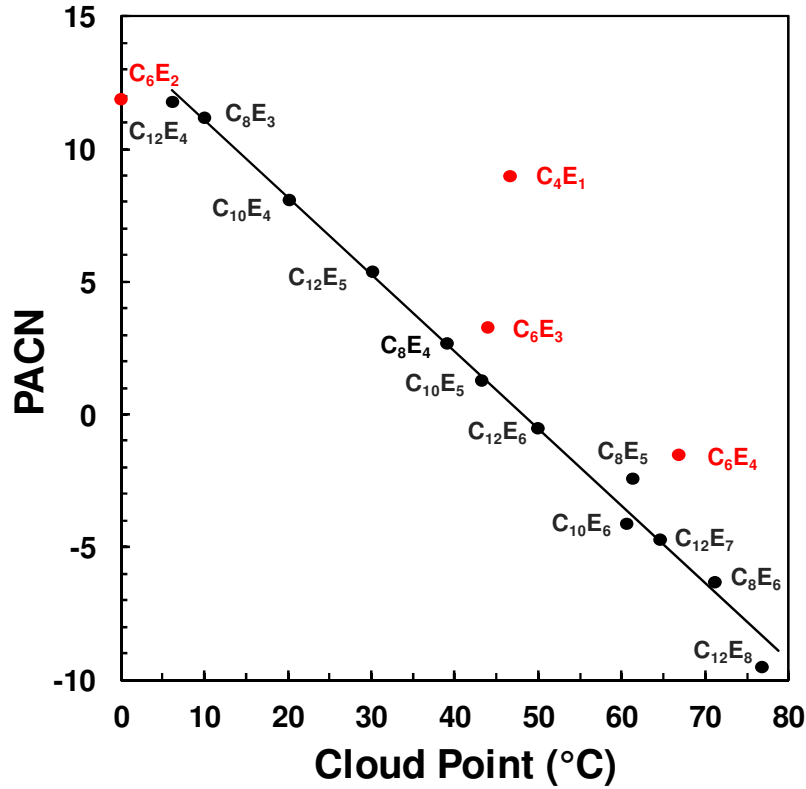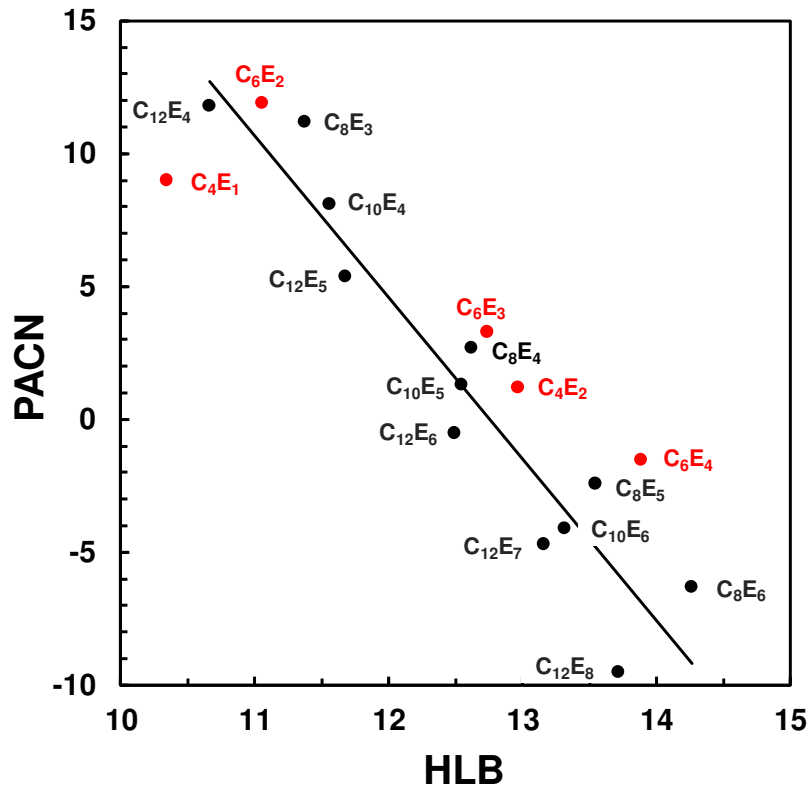
Figure 8. Linear correlation between the Preferred Alkane Carbon Number (PACN) of C_iE_j surfactants (black dots) or hydrotropes (red dots) and their HLB numbers.

A fairly good linear correlation ($R^2 = 0.90$) is obtained for the 12 true surfactants (black dots) whereas the red dots corresponding to the hydrotropes are somewhat appart the correlation line. The HLB scale therefore expresses only roughly the true amphiphilicity of surfactants, even for simple molecular structures such as C_iE_j. It should also be noted that the fish-tail-temperature method is applicable only to moderately hydrophilic surfactants whose HLBs are between 10 and 15. For surfactants that are either more hydrophilic (HLB > 15) or more lipophilic (HLB < 10) their amphiphilicity can be experimentally estimated by the PIT-slope-method. This new alternative method is based on the perturbation, provided by the surfactant under study, to the PIT of a reference system $C_{10}E_4$/n-Octane/Water [49,60].

5.1.3 PACNs vs Curvatures of the interfacial film

The curvature(s) of the amphiphilic film separating water-rich and oil-rich microdomains of a microemulsion is a key parameter for understanding the phase behaviour of C_iE_j/Oil/Water systems. Indeed, once known the evolution of the curvature(s) according to the scanning variable, it is in principle possible to determine the experimental conditions providing the optimum formulation and to predict the effectiveness of the surfactant for solubilising water and oil within the optimum microemulsion (i.e. the solubilisation ratio). In the regions of WI ($T < T_l$) and WII ($T > T_u$), the morphologies of the microemulsions are relatively simple since it can be considered, in a first approximation, as fluctuating swollen normal or inverted micelles characterized by a single mean curvature ($1/r$). On the other hand, in the WIII region, the microemulsion is bicontinuous and the complex geometry of the interfacial film may be described by the two principal curvatures c_1 and c_2 assuming the interfacial film to be infinitely thin (Helfrich's model). For more rigid microemulsions obtained when the WOR is very different from one or when the surfactants have long tails and/or ionic heads, the thickness of the interfacial film must be taken into account to assess the curvature energies of the interfacial film [92].

- *Experimental study of the interfacial film microstructure:*

In his landmark paper, Strey characterized experimentally the microstructure and the interfacial curvature of a series of microemulsions prepared from the model system $C_{12}E_5$/n-Octane/Water in a wide range of temperature from 5 to 65 °C [93]. The microstructures were observed by freeze fracture electron microscopy and the sizes of the O and W nano-domains were assessed by small-angle neutron scattering (SANS). He found that the "mean interfacial

curvature" H defined by equation (7) varies almost linearly with temperature according to Eq. 8 in the whole range of temperature from positive to negative values in the WI and WII regions respectively. Within the WIII region, H passes through a 0 value at the optimum temperature (T* = 32.6 °C) where the interfacial tension $\gamma_{o/w}$ exhibits a strong minimum.

"Mean Curvature"

$$H = (c_1+c_2)/2 \tag{7}$$

$$H = - 1.22.10^{-3}(T – T^*) \tag{8}$$

$$H = - 9.27.10^{-3} - 1.22.10^{-3}(T - 25) \tag{9}$$

Eq. 8 can be rearranged into Eq. 9 to bring out the similarity with the HLD_N equation (Eq. 4). It can thus be seen that for given surfactant and oil, the HLD_N value is, to within a constant, proportional to H over a wide temperature range around the optimum temperature T* as already shown by Kunz et al. [23]. Based on this single experimental observation, Acosta et al. have generalized the linear correlation by assuming that the mean curvature H changes proportionally to the HLD for both ionic [22] and nonionic surfactants [94]. Using this hypothesis, they developed the so-called Net-Average-Curvature (NAC) model which assumes that the three types of microemulsions (O/W, W/O and bicontinuous) can be represented as hypothetical spherical droplets of oil and water coexisting at the same time. This simple model can roughly predict many useful features of the C_iE_j/Oil/Water systems such as fish diagrams, interfacial tensions, droplets size as well as the characteristic length ξ of bicontinuous microemulsions.

A posteriori, the linearity of H vs. T is surprising since, for temperatures very far from T*, H (and thus HLD_N) should not vary linearly with T. Indeed, mean curvature of the interfacial film should exhibit a sigmoidal profile since it is expected to tend asymptotically towards the curvature of the fully hydrated normal micelle when T << T* and towards the curvature of the dehydrated reversed micelle when T >> T* [93]. However, within the temperature range examined experimentally (5 - 90°C), Fig. 4a-f show that the fish-tail-temperatures T* vary linearly as a function of the ACN of n-alkanes. We can therefore consider that equation 4 expressing the linear evolution of HLD_N as a function of T is also valid within the same temperature range. To illustrate this behaviour, the evolution of HLD_N as a function of T is represented in Fig. 9 for a series of C_iE_4/n-Octane/Water systems. The selected surfactants C_6E_4, C_8E_4, $C_{10}E_4$ and $C_{12}E_4$ have the same number of ethoxy groups and different chain lengths. This series of surfactants and this oil were chosen because it allows us to see the influence of the chain length on HLD_N and on the width of the WIII zone delimited by the two dotted curves
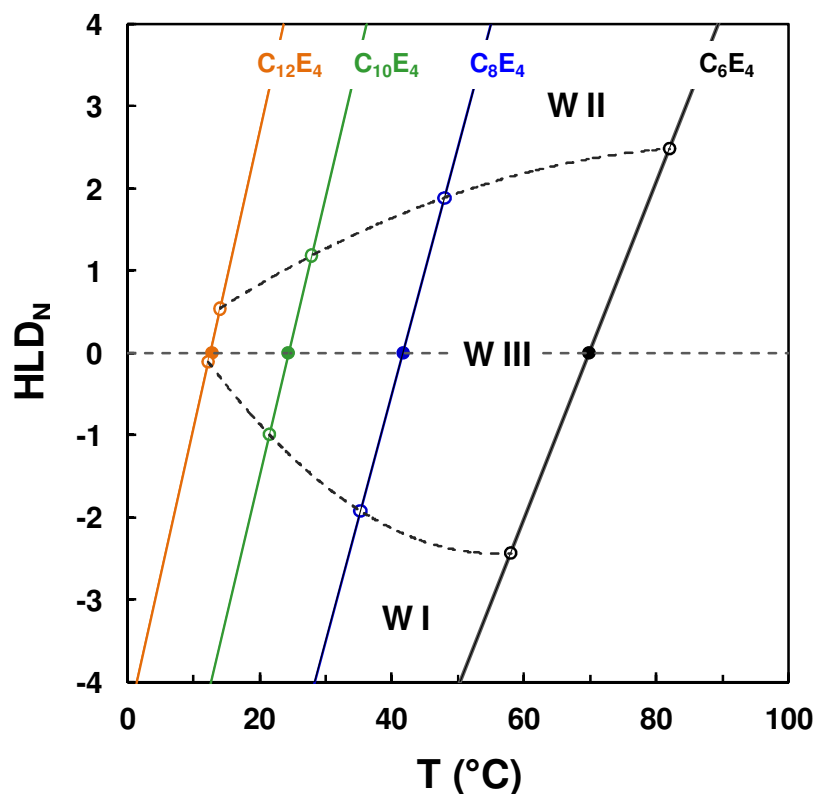
Figure 9. Linear evolution of HLD_N as a function of temperature for a series of C_iE_4/n-Octane/Water systems with i = 6, 8, 10 or 12. The filled points correspond to the fish-tail-temperatures T^* and the empty points to T_{low} and T_{up} taken from the literature [50,67].

5.1.4 PACNs vs PIT-slopes

A new procedure called the "PIT-slope method" has been proposed recently to quantify the amphiphilicity of any surfactant around 25 °C. It is based on the perturbation to the PIT of a reference system $C_{10}E_4$/*n*-Octane/Water, induced by the addition of increasing amount of the investigated surfactant [48]. This method is very versatile because it is applicable to all types of surfactants, ionic or nonionic, well-defined or technical grade [49]. Furthermore, unlike the fish-tail-temperature method, it makes it possible to characterize both water-insoluble hydrophobic surfactants and highly hydrophilic surfactants which would give, with the n-alkanes as oils, fish-tail-temperatures lower than 0. The characteristic quantity thus measured (dPIT/dx) is the slope of the straight line showing the evolution of the PIT as a function of the molar fraction of the added surfactant. A fairly good linear correlation (R^2 = 0.92) was found by Ontiveros et al. for the C_iE_j surfactants whose PACNs are known and which have been studied by the PIT-slope method [60]

6   Equivalent Alkane Carbon Number (EACN) of oils

6.1   Experimental determination of EACNs

The quantitative evaluation of the hydrophobicity of oils is extremely important because it guides the choice of the most effective surfactant for solubilising a given oil in water. This issue is encountered in various applications such as washing laundry for removing greasy stains [95] in cosmetics to remove makeup products deposited on the skin [96] in perfumery to design ethanol-free perfumes [97] in polymers for polymerization of monomers in mini- or micro- emulsions [81,98] or in the petroleum industry to formulate optimum microemulsions for EOR [99].

The oil hydrophobicity also plays a crucial role when one wants to design, by a rational approach, an emulsion having a predefined morphology [20]. Indeed, the decisive influence of the nature of the oils on the type of emulsion obtained by stirring a SOW system has been recognized since a long time by Bancroft [2,3] and then by Griffin [4] who attempted to quantify oil hydrophobicity by coining the concept of "required HLB" of oils. However, the values of "required HLB" published by Griffin [5] are too inaccurate to be applicable and, actually, this concept has hardly been applied by formulators, unlike the HLB scale which is still currently employed. During the early studies on EOR, Cash *et al.* addressed this issue by introducing the concept of Equivalent Alkane Carbon Number (EACN) of non-alkane oils [25] which was defined as the number of carbon atoms of the linear alkane exhibiting an equivalent hydrophobicity to the oil under study. The EACN is not necessarily an integer number, it is usually a fractional number which may even be negative for small polar oils such as short chain chlorinated solvents or esters.

At that time and still now, the EACN concept has been mainly applied to characterize different types of crude oils [24,100]. Then, it has been extended to other families of oils such as silicones [101], esters [32,34] , terpenes [30,35] and various perfume molecules [36,76].

Hexyl methacrylate was chosen as the oil to illustrate the method for determining the EACN because the position of its fish-tail-temperatures T^* has been precisely determined for a large series of C_iE_j by Lade *et al.* [81]. As shown in figure 4c, the T^* value of the C_8E_4/Hexyl methacrylate/Water system is plotted on the calibration straight line of the corresponding C_8E_4/*n*-Alkanes/Water systems in order to read on the X-axis the EACN value of this oil. For determining the EACN, a judicious choice of the surfactant is crucial for both practical and theoretical reasons. The shorter the chain of the surfactant, the higher its monomeric concentration in the excess water and oil phases [50]. Accordingly, the interfacial film of

surfactants is no longer in equilibrium with pure water and pure oil as it should ideally be. The presence of some C_iE_j in one or both of the excess phases may therefore influence the apparent EACN of the oil under study. In this respect, $C_{12}E_j$ surfactants could appear preferable since they dissolve less than shorter C_iE_j surfactants in the excess phases. However, SOW systems based on $C_{12}E_j$ surfactants require several days or weeks to equilibrate and often form liquid crystals that further slow down the attainment of equilibrium and complicate Winsor type identification. In contrast, SOW systems based on $C_{10}E_j$ surfactants require only a few hours to reach equilibrium and those based on C_8E_j surfactants, a few minutes. Accordingly, the three surfactants C_8E_3, C_8E_4 and C_8E_5 are the best compromise for determining T* because they are commercially available and allows a quick EACN determination of both highly hydrophobic oils, as well as very polar ones as shown in Table 4. The EACN concept is of interest only if the values assigned to oils do not depend on the nature of the C_iE_j surfactant used for its measurement. This key issue has been checked by Queste *et al.* who showed that for a number of chemically different oils, i.e. dibutylether, isopropyl myristate, squalane and dodecylbenzene, EACNs calculated from the T*-values determined by different authors were akin regardless of the C_iE_j used [31]. Similarly, Bouton *et al.* checked that the EACN values of 26 terpenes and complex (branched, unsaturated, cyclic) hydrocarbons were identical to within 0.5 unit using either C_6E_4, C_8E_4 or $C_{10}E_4$ indifferently [30,33] However, for very polar oils, two major problems might decrease the accuracy of their EACN measurement. The first one stems from the fact that for oils having an EACN lower than 6, the calibration curve established with *n*-alkanes must be extrapolated to the dotted parts of the inclined lines in figures 4a-e. Accordingly, the lower the EACN, the greater the uncertainty over its estimated value. The second problem, already discussed above, arises from the monomeric solubility of the nonionic PEO surfactant in the oil phase which increases its apparent polarity and therefore decreases its measured EACN. For examining how these two issues influence the EACN, the EACN values of hexyl methacrylate determined with 9 different C_iE_j (see the red empty dots shown in figures 4b-e) were compared. We found an average value of EACN equal to 0.1 with a standard deviation of 0.7. However, we observe that the EACN-values slightly decrease when j increases for a given i value. This behaviour is readily explained by the fact that solubilized C_iE_j increases all the more the apparent polarity of the oil that the number of ethoxylated units is high. In conclusion, the uncertainty on the EACN values is all the greater as the EACN is low but the assumption of giving a single value for the EACN of oil remains acceptable. All these

phenomena make the measurement of the EACNs of very polar oils such as ethers, esters, ketones, nitriles or acrylic monomers less accurate than that of hydrocarbons and terpenes.

6.2 EACNs inferred from published fish-tail-temperatures

All the fish-tail-temperatures T* reported in the literature for true ternary C_iE_j/Oil/Water systems as well as assessed EACN values are summarized in Table 4. Given the different sources of inaccuracies mentioned above, we estimate that the uncertainties on the EACN values are approximately equal to 1.0, 0.5 and 0.2 when EACN is < 0 or between [0-6[and [6-16] respectively .

Table 4. Fish-tail-temperature T* reported in the literature for true ternary systems C_iE_j/Oil/Water. Average EACN values of the oils are determined from the calibration straight lines shown in figure 4. Fish-tail-temperatures of *n*-alkanes are reported in Tables 1 and 2.

N°	Oil	N_C	i	j	T*/°C	C_o/%	C*/%	EACN	Ref
				Branched and cyclic alkanes					
1	Cyclohexane	6	6	4	46.5		32.9	2.4	[102]
1	Cyclohexane	6	8	4	20.7			1.7	[102]
1	Cyclohexane	6	8	4	21.0	2.5	14.8	1.8	[68]
1	Cyclohexane	6	6	3	21.5	3.1	24.2	2.5	[103]
1	Cyclohexane	6	10	6	38.2	1	6.9	-	[103]
1	Cyclohexane	6	10	8	58.7	1.6	8.4	-	[103]
2	Methylcyclohexane	7	6	4	52.3		37.8	3.5	[102]
2	Methylcyclohexane	7	8	4	24.4			2.8	[102]
3	1,4-Dimethylcyclohexane	8	6	4	58.4		41	4.6	[102]
3	1,4-Dimethylcyclohexane	8	8	4	30			4.5	[102]
4	Ethylcyclohexane	8	6	4	57.8		40.4	4.5	[102]
4	Ethylcyclohexane	8	8	4	29.7			4.5	[102]
4	Ethylcyclohexane	8	10	4	13		5.8	3.7	[31]
5	Cyclooctane	8	6	4	55.5		34	4.1	[35]
6	1,2-Dimethylcyclohexane	8	6	4	54.6		38.8	3.9	[31]
6	1,2-Dimethylcyclohexane	8	8	4	23.7			2.6	[102]
7	Propylcyclohexane	9	6	4	65		47.4	5.8	[102]
7	Propylcyclohexane	9	8	4	35.9			6.3	[102]
7	Propylcyclohexane	9	10	4	18		9.7	5.5	[31]

8	Isopropylcyclohexane	9	6	4	63.8		46.7	5.6	[102]
8	Isopropylcyclohexane	9	8	4	33.8			5.7	[102]
8	Isopropylcyclohexane	9	10	4	15.2			4.5	[102]
9	Butylcyclohexane	10	6	4	72.4		52.2	7.2	[102]
9	Butylcyclohexane	10	8	4	41.1			7.9	[104]
9	Butylcyclohexane	10	10	4	22	1.8	11	6.9	[31]
10	Cyclodecane	10	6	4	63.9		38	5.6	[37]
11	cis-Decalin	10	6	4	62.3		40	5.3	[37]
12	Myrcane	10	6	4	88.1		60.9	10.0	[30,33]
12	Myrcane	10	8	4	51.8		35	11.2	[34,35]
12	Myrcane	10	10	4	31			10.1	[102]
13	Pinane	10	6	4	56.8		37.3	4.3	[34,35]
13	Pinane	10	8	4	27.7		18.3	3.9	[34,35]
14	p-Menthane	10	6	4	66.9		46.9	6.2	[34,35]
14	p-Menthane	10	8	4	37		23.4	6.7	[34,35]
14	p-Menthane	10	10	4	15.6			4.6	[34,35]
15	Decylcyclohexane	16	10	4	43		22.8	14.4	[112]
16	Dodecylcyclohexane	18	10	4	51.5		25.7	17.5	[31]
17	Squalane	30	10	4	71		39	24.5	[112]
	Halogenated Alkanes								
18	Carbon tetrachloride	1	10	8	23.0	5.0	6.5	-	[105]
19	1-Bromo-3-methylpropane	4	6	4	14.8			-3.4	[37]
20	1-Chlorooctane	8	12	5	12.8	2.4	7.2	1.0	[114]
21	1-Chlorodecane	10	10	4	12.5		10	3.5	[37]
22	1,10-Dichlorodecane	10	12	5	27.7	3.8	30.4	6.3	[106]
23	1-Chlorododecane	12	10	4	18.5		14	5.6	[37]
23	1-Chlorododecane	12	12	5	26.3	2.1	7.7	5.8	[114]
24	1-Chlorotetradecane	14	10	4	25		17	8.0	[37]
24	1-Chlorotetradecane	14	12	5	30.3	2	8.8	7.3	[114]
25	1-Chlorohexadecane	16	10	4	30		23	9.8	[37]
25	1-Chlorohexadecane	16	12	5	35.2	1.8	10.7	9.0	[114]

Alkenes, Terpenes, Alkynes and Aromatics

26	Cyclohexene	6	6	4	26.5		22.2	-1.2	[102]
27	1,3-Cyclohexadiene	6	6	4	16.2		30.3	-3.1	[102]
28	1,4-Cyclohexadiene	6	6	4	11.1		23.7	-4.0	[102]
29	1-Methyl-1-cyclohexene	7	6	4	37.4		31	0.8	[102]
29	1-Methyl-1-cyclohexene	7	8	4	12.4			-0.8	[102]
30	4-Methyl-1-cyclohexene	7	6	4	36.3			0.6	[102]
30	4-Methyl-1-cyclohexene	7	8	4	13.2			-0.5	[102]
31	3-Methyl-1-cyclohexene	7	6	4	35.3		28.2	0.4	[102]
31	3-Methyl-1-cyclohexene	7	8	4	10.5			-1.4	[102]
32	2,5-Norbornadiene	7	6	4	15.4		23	-3.2	[102]
33	Toluene	7	10	8	24.3	7.9	11.4	-	[103]
34	1-Octene	8	6	4	54.6		42	3.9	[37]
35	cis-Cyclooctene	8	6	4	41.6		26	1.5	[37]
36	1-Octyne	8	6	4	23.3		24	-1.8	[37]
37	m-xylene	8	12	8	24			-	[78]
38	p-Xylene	8	6	4	20.2		24	-2.4	[37]
38	p-Xylene	8	12	8	25.8	5.2	7.7	-	[30]
39	Ethylbenzene	8	10	8	33.2	6.5	10.9	-	[111]
39	Ethylbenzene	8	12	8	24			-	[83]
40	1-Decene	10	6	4	63.2		44	5.5	[37]
41	1-Decyne	10	6	4	33.8		25	0.1	[37]
42	Butylbenzene	10	6	4	35.2		27	0.4	[37]
43	Phenyl-1-butyne	10	6	4	15.1		28	-3.3	[37]
44	α-Pinene	10	6	4	52.7	2	35.3	3.6	[34,35]
44	α-Pinene	10	8	4	26.1		18.1	3.4	[34,35]
45	p-Menth-2-ene	10	6	4	50			3.1	[30]
45	p-Menth-2-ene	10	8	4	26.9		17.2	3.6	[34,35]
46	Δ-3-Carene	10	6	4	48.8		33.9	2.9	[34,35]
46	Δ-3-Carene	10	8	4	21.7		18.4	2.0	[34,35]
47	β-Pinene	10	6	4	45.8		31.5	2.3	[34,35]
47	β-Pinene	10	8	4	21.7		18	2.0	[34,35]
48	Limonene	10	6	4	44.3		28.4	2.0	[34,35]
48	Limonene	10	8	4	20.4		16.2	1.6	[34,35]

48	Limonene	10	12	8	46			-	[83]
49	γ-Terpinene	10	6	4	43.3		28.7	1.9	[34,35]
49	γ-Terpinene	10	8	4	19.6		17.8	1.4	[34,35]
50	α-Terpinene	10	6	4	41.1		28.9	1.5	[34,35]
50	α-Terpinene	10	8	4	17.7		18.3	0.8	[34,35]
51	Terpinolene	10	6	4	40.5		29.7	1.3	[34,35]
51	Terpinolene	10	8	4	15.3		17.7	0.1	[34,35]
52	p-Cymene	10	6	4	31.6		25.9	-0.3	[34,35]
52	p-Cymene	10	8	4	10.8		17.4	-1.3	[34,35]
53	Butylbenzene	10	12	8	38			-	[83]
54	1-Dodecene	12	6	4	77.7		55	8.1	[37]
55	1-Dodecyne	12	6	4	44		30	2.0	[37]
56	Hexylbenzene	12	12	8	50			-	[83]
57	1-Tetradecyne	14	6	4	54.3		34	3.9	[37]
58	Octylbenzene	14	10	4	14		11.8	4.0	[31]
59	2,6,10-trimethyl undecane-2,6-diene	14	8	4	49	2.5	30.2	10.3	[34,35]
60	Longifolene	15	6	4	69.5			6.6	[34]
60	Longifolene	15	8	4	38.9		26.2	7.3	[34,35]
61	Caryophyllene	15	6	4	64.1		43.5	5.7	[34,35]
61	Caryophyllene	15	8	4	35.5	2.5	23.8	6.2	[34,35]
62	Decylbenzene	16	10	4	19.5		16.2	6.0	[32]
63	1-Octadecene	18	10	4	42.4		37	14.2	[37]
64	Dodecylbenzene	18	10	4	24.5	6	19.2	7.8	[32]
64	Dodecylbenzene	18	12	8	70			-	[83]
65	Squalene	30	10	4	41.3		31.9	13.8	[38]
Ethers, Esters, Nitriles and Ketones									
66	Diisopropylether	6	12	6	32.5	3	10.5	2.2	[107]
67	Dibutylether	8	6	4	46.3		31	2.4	[38]
67	Dibutylether	8	10	4	12		11.5	3.3	[32]
67	Dibutylether	8	12	6	35.5	3	8	3.2	[115]
68	2-Octanone	8	6	4	14.6		22	-3.4	[38]
69	Octanenitrile	8	6	4	23.7		30	-1.7	[38]

70	Dipentylether	10	6	4	56.3		39	4.2	[38]
71	C_3-O-C_4-O-C_3	10	12	6	31.7	5	12	1.9	[115]
72	C_4-O-C_2-O-C_4	10	12	6	31.2	5	12.2	1.7	[115]
73	2-Decanone	10	6	4	21.8		22	-2.1	[38]
74	Decanenitrile	10	6	4	30.1		30	-0.6	[38]
75	2-Undecanone	11	6	4	25.8		23	-1.3	[38]
76	Ethyl decanoate	12	6	4	43		28.3	1.8	[104]
76	Ethyl decanoate	12	10	4	9.2		14.3	2.3	[34]
76	Ethyl decanoate	12	12	6	32.5		11.6	2.2	[37]
77	Dihexylether	12	6	4	67.3	7	47	6.2	[38]
78	2-Dodecanone	12	6	4	29.8	15	24	-0.6	[38]
79	Dodecanenitrile	12	6	4	35	14	31	0.3	[38]
80	Ethyl dodecanoate	14	10	4	13.4		15	3.8	[36]
81	Decyl butyrate	14	10	4	16.8		16.6	5.0	[36]
82	Hexyl octanoate	14	10	4	20.1		17.5	6.2	[36]
83	Diheptylether	14	6	4	76.9		54	8.0	[38]
84	Ethyl myristate	16	10	4	17.4		16.1	5.2	[36]
85	Butyl dodecanoate	16	10	4	22.8		17.6	7.2	[36]
86	Octyloctanoate	16	10	4	25.2		19.3	8.1	[36]
87	Dioctylether	16	6	4	89.5		58	10.3	[38]
88	Myristyl propionate	17	10	4	21.6		17.8	6.8	[36]
89	Isopropyl myristate	17	10	4	22.9	3.5	16.9	7.2	[36]
89	Isopropyl myristate	17	10	4	23		19.5	7.3	[32]
90	Ethyl palmitate	18	10	4	21.6		16.4	6.8	[36]
91	Hexyl dodecanoate	18	10	4	28.8		21.9	9.3	[34]
92	Ethyl oleate	20	10	4	23		17.7	7.3	[36]
92	Ethyl oleate	20	10	4	22.5		17.0	7.1	[108]
93	Bis(2-ethylhexyl) adipate	22	10	4	29.7		25.9	9.7	[36]
94	Tricaprilin	27	10	4	36.8	6.8	31.8	12.2	[36]
95	Tricaprin	33	10	4	41.3	6	33	13.8	[36]
95	Tricaprin	33	10	4	38.9		31	13.0	[32]
96	Trilaurin	39	10	4	46.6		37.3	15.7	[33]
97	Trimyristin	45	10	4	54.4		42.9	18.5	[33]

98	Tripalmitin	51	10	4	61.7		52	21.2	[33]
99	Tristearin	57	10	4	69.4		57.9	23.9	[33]
100	Triolein	57	10	4	61.8	9	51.5	21.2	[33]
	Fragrances, acrylates and miscellaneous								
101	Methyl methacrylate	5	10	6	9	8.30	16.80	-	[81]
102	Ethyl methacrylate	6	10	6	16.4	7.60	15.70	-	[86]
103	Butyl methacrylate	8	10	6	26.4	6.30	14.70	-	[86]
104	2-Ethylhexanol	8	12	8	17			-	[83]
105	Benzyl acetate	9	12	8	29			-	[83]
106	Menthone	10	6	4	24.8		27.7	-1.5	[112]
107	Eucalyptol	10	6	4	24.4		21.3	-1.6	[112]
108	Rose oxide	10	6	4	23.6		24.9	-1.7	[112]
109	D-Carvone	10	6	4	16		24.9	-3.1	[112]
110	Linalool	10	12	8	9.5	15	25.6	-	[112]
110	Linalool	10	12	8	10			-	[83]
111	Hexyl methacrylate	10	6	3	13		24.8	0.4	[86]
111	Hexyl methacrylate	10	6	4	32.1	12.3	25.1	-0.2	[86]
111	Hexyl methacrylate	10	6	5	46.3	12.1	26.0	-	[86]
111	Hexyl methacrylate	10	8	4	14.6	6.7	19.0	-0.1	[86]
111	Hexyl methacrylate	10	8	5	30.6	6.8	19.1	-0.8	[86]
111	Hexyl methacrylate	10	10	4	4.8		12.8	0.7	[86]
111	Hexyl methacrylate	10	10	5	20.6	5.1	13.9	-0.2	[86]
111	Hexyl methacrylate	10	10	6	33.4	5.6	14.6	-	[86]
111	Hexyl methacrylate	10	10	7	43.1	5.8	15.2	-	[86]
111	Hexyl methacrylate	10	10	8	51.5	5.8	15.5	-	[86]
111	Hexyl methacrylate	10	12	5	14.4	4.3	9.2	1.5	[86]
111	Hexyl methacrylate	10	12	6	26.9	4.5	10.2	0.2	[86]
111	Hexyl methacrylate	10	12	7	37.3	4.6	10.5	-0.4	[86]
111	Hexyl methacrylate	10	12	8	46.1	4.8	11.3	-	[86]
111	Hexyl methacrylate	10	12	9	53.1	5.0	12.6	-	[86]
111	Hexyl methacrylate	10	14	7	32.6	4.1	7.6	-	[86]
111	Hexyl methacrylate	10	14	8	41.4	4.1	8.1	-	[86]
112	Octyl methacrylate	12	10	6	40.4	4.7	15.0		[86]

113	Menthyl acetate	12	6	4	32.5		24.4	-0.1	[36,104]
114	Citronellyl acetate	12	6	4	31.9		25.2	-0.2	[38,112]
115	Geranyl acetate	12	6	4	29.9		25.5	-0.6	[38,112]
116	Linalyl acetate	12	6	4	28.4		24.8	-0.9	[38,112]
117	α-Damascone	13	6	4	26.3		26.4	-1.3	[112]
118	Methyl dihydrojasmonate	13	6	4	23.8		25.8	-1.7	[112]
119	β-Ionone	13	6	4	23		24.8	-1.9	[104]
119	β-Ionone	13	12	8	39			-	[83]
120	α-Hexylcinnamic aldehyde	15	12	8	39			-	[83]
121	Ethylene brassylate	15	6	4	27.4		26.4	-1.1	[112]
122	Methyl cedrylether	16	6	4	52.1		33.2	3.5	[112]
123	Ambrettolid	16	6	4	38.6		27.6	1.0	[112]
124	Dodecyl methacrylate	16	10	6	49.9	3.6	17.4	-	[86]
125	Hexadecyl methacrylate	20	10	6	57.2	2.4	20.3	-	[86]

6.3   Structural effects on EACNs

The values of the EACNs of oils mainly depend on their polarity and their carbon numbers as highlighted in Figure 10 showing the evolution of EACN values for different homologous series of oils according to the number of carbon atoms N_C. The Figure 10a presents data for hydrocarbons (alkanes, alkenes, alkynes and aromatics) and Figure 10b for polar oils (ethers, chloroalkanes, esters, nitriles and ketones). A number of general tendencies with regard to the effect of structural modifications on the EACNs of oils are summarized in Table 5 by taking the C_{12} oils as references.
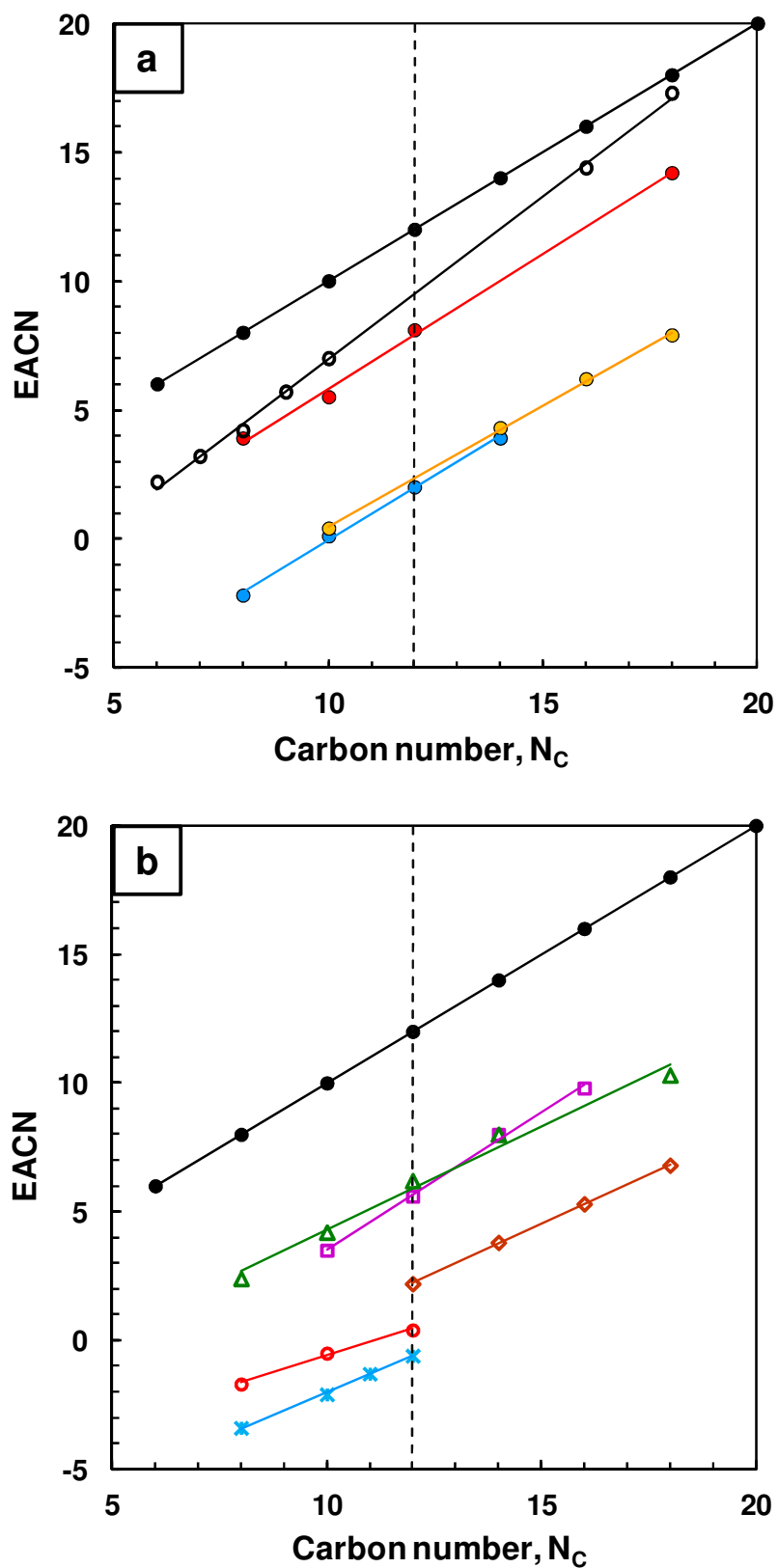
Figure 10. Evolution of the EACN values vs Carbon Number for several homologous families. The dashed lines indicate the C_{12} oils as references.

(a) Hydrocarbons: (●) n-alkanes, (○) n-alkylcyclohexanes, (●) 1-alkenes, (●) n-alkylbenzenes, (●) 1-alkynes.

(b) Polar oils : (△) dialkyethers, (□) 1-chloroalkanes, (◇) ethyl alkanoates. (○) 1-nitriles, (✳) 2-ketones.

Table 5. Influence of various structural modifications on EACNs of C_{12}-hydrocarbons (n-alkanes, *n*-alkylcyclohexanes, 1-alkenes, 1-alkynes and n-alkylbenzenes) and C_{12}-functionalized oils (dialkyethers, 1-chloroalkanes, ethyl alkanoates. 1-nitriles, 2-ketones). *n*-Dodecane is used as a reference oil to calculate ΔEACN.

Structural modifications	Examples	ΔEACN
Homologation (+ 1 CH_2)	alkanes, alkenes, alkynes, aromatics, chloroalkanes	+ 1.0
Homologation (+ 1 CH_2)	n-alkylcyclohexane	+ 1.3
Homologation (+ 1 CH_2)	ketones, ethers, esters	+ 0.7/0.8
Homologation (+ 1 CH_2)	nitriles	+ 0.5
Branching ($CH_2 \rightarrow CH_3$)	squalane	- 0.9
Cyclisation	C_6, C_8 and C_{10} cycloalkanes	- 4.0
Terminal double bond	1-alkenes	- 4.1
Terminal triple bond	1-alkynes	- 10.0
Aromatisation	n-alkylbenzenes	- 9.7
Ether group	dialkylethers	- 6,1
Chlorination	1-chloroalkanes	- 6,3
Ester group	ethyl alkanoates	- 9,8
Nitrile group	1-nitriles	- 11,6
Ketone group	2-ketones	- 12,6

Influence of the length of homologous oils on EACN values. Figure 10a shows that the evolution of EACNs of different homologous families of oils is linear with respect to their total number of carbon atoms (N_C). *n*-Alkanes are used as reference oils to calibrate the EACN scale since, by definition, ACN = Nc. The first thing to note is that EACNs of all non-linear hydrocarbons as well as functionalised oils are lower than ACNs of *n*-alkanes having the same number of carbon atoms. Interestingly, the straight lines corresponding to 1-alkenes, 1-alkynes, *n*-alkylbenzenes and 1-chloroalkanes are parallel to the straight line of *n*-alkanes whereas EACNs of *n*-alkylcyclohexanes approximates the ACNs of *n*-alkanes when N_C increases. This means that long *n*-alkylcyclohexanes ($N_C \gtrsim 20$) have roughly the same influence on the phase behaviour as the *n*-alkanes having the same N_C. In contrast, the extension of the hydrocarbon chain of polar oils such as ethers, esters, nitriles and ketones increases their EACNs by less than one unit per methylene group.

Influence of branching and cyclisation on EACN values. Branched alkanes are known to exhibit slightly lower EACNs than their linear isomers. For instance, the EACN of the triterpene squalane is 24.4 whereas it is 30.0 for its n-C_{30} isomer, *n*-triacontane. Cyclisation of the chains leads to a stronger decrease of EACN (ΔEACN ≈ - 4). For instance, cyclohexane is

known since a long time to behave as a shorter alkane than *n*-hexane as shown by the position of the fish diagrams in Figure 3 [103]. This behaviour is also observed for C_8 and C_{10} cycloalkanes compared to their respective linear isomers.

Unsaturation and aromatisation. EACNs dramatically decrease with the number of unsaturations. Indeed, the introduction of a double or a triple bond at the end of an n-alkyl chain decreases the EACN value by 4 and 10 units respectively as shown by comparing 1-alkenes and 1-alkynes with n-alcanes (Fig. 10a and Table 4). In the same way, the introduction of one endocyclic double bond into the p-menthane skeleton diminishes the EACN value by 2.5 units. A second double bond leads to a further decrease by about 2 EACN units. However, the position of the double bond and the structure of the starting skeleton have also a significant influence. Endocyclic double bonds have a lower influence on the final EACN value than exocyclic double bonds. Actually, β-pinene has a significantly lower EACN (1.9) than pinane (3.4) whereas the EACN value of α-pinene (3.0) is only slightly lower. Aromatic hydrocarbons such as p-cymene (EACN = -0.4) behave as much polar oils than the corresponding cyclohexanes, i.e. p-menthane (EACN = +6.0). In the same way, the comparison of the series of n-alkylbenzenes and n-alkylcycloalkanes shows that the aromatization of the C_6-cycle induces a decrease of EACN ranging from -6 to -9 depending on the length of the alkyl chain.

Functionalised oils. EACN values strongly depends on the type and position of the functional group attached to the alkyl chain [34]. By comparing EACNs for oils of similar length – C_{12} for instance –, but with different functional groups, one can classify them according to their affinity for the interfacial film: 2-ketones > 1-nitriles > ethyl alkanoates ≈ 1-alkynes ≈ n-alkylbenzenes > 1-chloroalkanes ≈ dialkylethers > 1-alkenes > n-alkylcyclohexanes > i-alkanes > n- alkanes.

These general rules are sufficient to roughly estimate EACNs of unknown monofunctional oils. Nevertheless, they are useless to predict EACNs of more complex oils such as terpenes, fragrance molecules, triglycerides or monomers for which several structural modifications (branching, cyclization, aromatisation, polyfunctionalisation) are simultaneously involved. For such oils one must resort to more sophisticated predictive models that can correlate their molecular structures to their EACN values. An effective approach based on the COSMO-RS theory will be presented below in a specific section of this review.

6.4 EACNs of mixed oils and segregation phenomena

Most industrial applications of SOW systems use oils mixtures. Actually, important natural oils such as edible oils, essential oils and crude oils are complex mixtures of triglycerides, terpenes or hydrocarbons, respectively. Similarly, synthetic oils such as fragrance oils and cosmetic emollients consist of a skilful blend of several components to optimize the sensory effects [109]. To emulsify, micro-emulsify or solubilise such oils, it is important to know whether the EACN of the mixed oils is simply equal to the weighted sum of the EACNs of the components or if interaction or segregation phenomena induce a non-ideal behaviour. Several reliable works report the fish-tail-temperature (T*) or the phase inversion temperature (PIT) of SOW systems with binary mixtures of oils and well-defined C_iE_j surfactants. Table 6 presents the studied oil blends and reports the maximum difference $\Delta T_{max} = (T_{exp}-T_{ideal})_{max}$ between the experimental temperature T_{exp} and the calculated temperature T_{ideal}. assuming an ideal behaviour. Similarly, $\Delta EACN_{max} = (EACN_{exp}- EACN_{ideal})$ is also calculated.

Table 6. C_iE_j/Mixed oils/Water systems whose optimum formulations are detected either by the fish-tail-method (T*) or by the PIT-method. $\Delta EACN$ represents the difference between the EACNs of two mixed pure oils ($EACN_{less\ polar}$ - $EACN_{more\ polar}$) whereas ΔT_{max} and $\Delta EACN_{max}$ are the maximum differences between experimental and calculated values assuming an ideal behaviour.

Less polar oil	More polar oil	$\Delta EACN$	Surfactant	Method	ΔT_{max} / °C	$\Delta EACN_{max}$	Ref.
Cyclohexane	Toluene	-	$C_{10}E_6$	T*	- 8	-	[103]
Cyclohexane	Toluene	-	$C_{10}E_8$	T*	- 7	-	[103]
n-Decane	Triolein	-11.1	$C_{10}E_4$	T*	+ 14	+5.0	[32]
n-Decane	Butyl dodecanoate	+2.8	$C_{10}E_4$	PIT	- 2.9	-1.1	This work
n-Decane	Hexyl octanoate	+3.3	$C_{10}E_4$	PIT	- 3.6	-1.2	This work
n-Decane	Ethyl myristate	+4.7	$C_{10}E_4$	PIT	- 4.2	-1.5	This work
n-Decane	Decyl butyrate	+5.0	$C_{10}E_4$	PIT	- 4.5	-1.5	This work
n-Decane	Ethyl dodecanoate	+6.2	$C_{10}E_4$	PIT	- 5.3	-1.8	This work

The fish-tail-temperature T* of mixed oils has been reported for different ratios of Cyclohexane/Toluene mixtures using pure $C_{10}E_6$ and $C_{10}E_8$ as surfactants [103] and for the mixture Triolein/*n*-Decane with $C_{10}E_4$ [32]. The non-ideal evolutions of T* according to the molar fraction of toluene or *n*-decane clearly appear in the figure 11, indicating a non-linearity

in optimum formulation with several oil mixtures. This is similar to what was found by Graciaa et al. with a mixture of ethyl oleate and hexadecane an a technical grade nonionic surfactants [28]. The present behaviour clearly indicates that this departure from linearity is occurring as a general rule even with pure surfactants and is thus definitively depending of some segregation in the mixture of oil species.
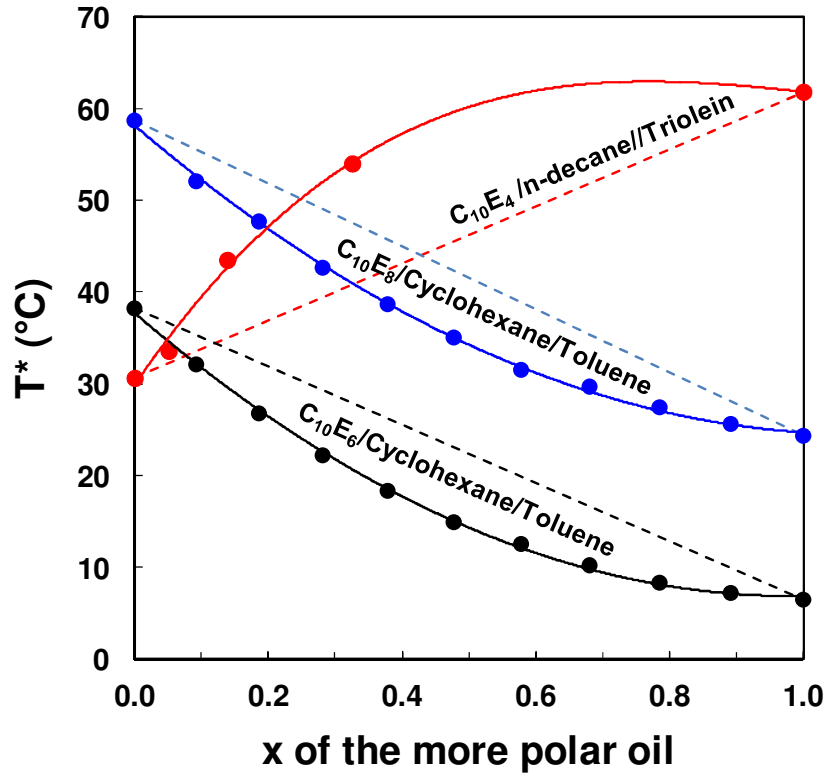

Figure 11. Fish-tail-temperatures of mixtures of cyclohexane and toluene at different molar fractions of the more polar oil using either (●) $C_{10}E_8$ or (●) $C_{10}E_6$ as surfactants [103]. Fish-tail-temperatures of mixtures of triolein and n-decane at different molar fractions using (●) $C_{10}E_4$ as surfactant [32]. The dotted line indicates the hypothetical linear behaviour of fish tail temperature as a function of oil composition.

The non-ideality of the fish-tail-temperature for an oil mixture, and therefore its EACN, is clearly dependent on the nature and the ratio of oils. Thus, the T* value of the mixture Triolein/*n*-Decane with a 33/67 molar ratio (T* = 54°C) is close to that of pure triolein (T* = 62°C) and much higher than the expected value (T* = 41°C) for an ideal mixture. It is clear that the deviation from linearity larger (see $\Delta EACN_{max}$ in table 6) is even greater when the difference in the polarity of the oils $\triangle EACN$ is larger. This deviation can be positive or negative depending on the EACN of the more polar oil. If the EACN of the polar oil is the highest, e.g. triolein/decane, T* value of the mixture as well as its EACN is higher than T* predicted by a linear fit. However, in most cases, the EACN of the polar oil is the lower, e.g. cyclohexane/toluene, and the experimental T* of the mixture is lower than the linear fit (Table

6). In order to further study the influence of the EACN difference on the non-ideality, we determined the PIT of mixtures of n-decane with five different ester oils of lower EACN at WOR = 1 in the presence of 7 wt.% of $C_{10}E_4$. Figure 12 shows the difference between the experimental PIT and the hypothetical ideal PIT for different n-decane/ester ratios, $\Delta PIT = PIT_{exp}-PIT_{ideal}$.
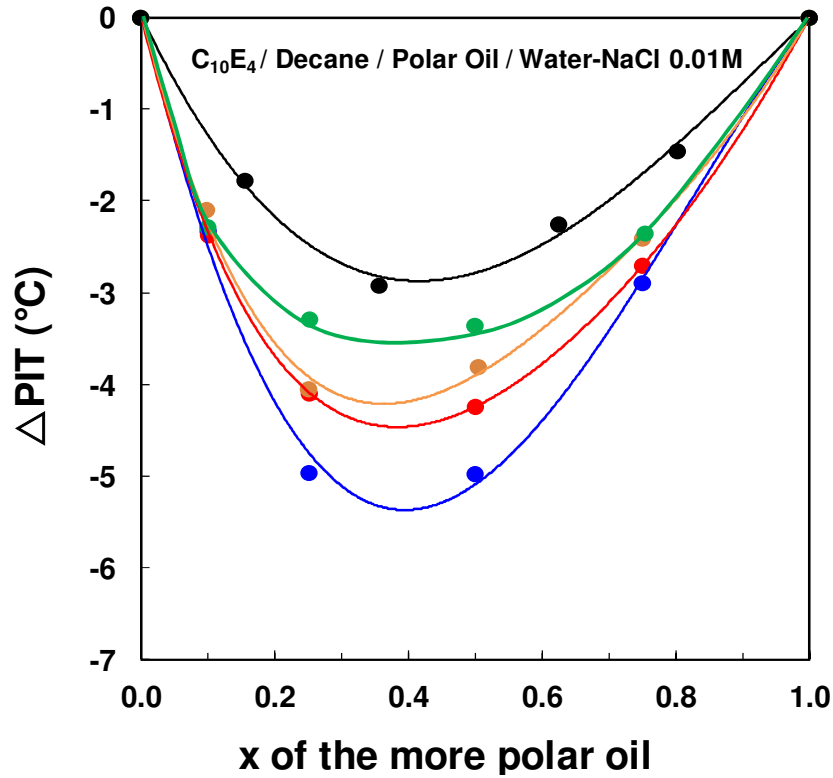
Figure 12. Difference between the experimental and the "ideal" PIT of the stirred emulsion consisting of the SOW system: 7 wt% $C_{10}E_4$/(Decane+Ester)/H_2O, NaCl 0.01M at WOR = 1. Five different esters were investigated: (●) ethyl dodecanoate, (●) decyl butyrate, (●) ethyl myristate, (●) hexyl octanoate and (●) butyl dodecanoate.

The physicochemical behaviour of these mixtures appears closer to that of the more polar oil than expected if the mixture is ideal. Actually, in all cases, experimental PITs and therefore EACNs of the mixtures are significantly lower than the predicted values assuming ideal mixtures (Table 6). The maximum deviations between the experimental EACN and the calculated from a linear approach ($\Delta EACN_{max}$) for the mixtures occur for a molar fraction close to 0.4 and vary from -1.1 (butyl dodecanoate) to -1.8 (ethyl dodecanoate). It is worth to note that the magnitude of the deviation increases with the difference between the EACN of the pure oils. The data of Engelskirchen [32] at equilibrium confirms this fact, for the decane/triolein system, the $\Delta EACN$ is -11.1 and the maximum deviation ($\Delta EACN_{max}$) is +5.0. An explanation for this behaviour was proposed by Graciaa *et al.* [28] with mixtures of

hexadecane (ACN=16) and ethyl oleate (EACN=7.3) in systems with ethoxylated surfactants. They demonstrated that the more polar oil, ethyl oleate, tends to accumulate in the interface vicinity. So, the oil layer located near the interface exhibits a composition different from that of the bulk oil in agreement with figures 11 and 12. In line with the above, Tchakalova *et al.* measured the PIT of $C_{10}E_5$/Oil/Water systems where the oil was either *n*-decane or isopropyl myristate to which was added a small amount (6%) of various oils, specially perfumery raw materials [38,76]. Their experimental results also showed systematic deviations from linearity.

When one of the oil of the mixture is amphiphilic (alcohol, amine, amide, asphaltene ...), the EACN value of the mixture is not enough to describe the physicochemical behaviour of SOW systems [110]. Actually, the amphiphilic oil molecules localized at the interface acts more like surfactants whereas those in the bulk modify the nature of the oil. Therefore, Ghayour *et al.* proposed to take into account both effects, i.e. a change into the EACN of the oil and into the PACN of the surfactant [111].

7   Interpretation of EACNs with the Effective-Packing-Parameter concept

Microemulsions consist of oil and water domains separated by an interfacial surfactant monolayer. This film divides space into the volume fractions demanded by the three constituents while optimising the packing of the amphiphilic molecules within the film. The type of microstructure (W/O, O/W or bicontinuous) is thus determined by the WOR and by the distribution of the surfactant between water, oil and the interfacial film. At each temperature, the surfactant film has a specific spontaneous curvature H_0 which usually differs from the mean curvature H defined by the equation (7). The difference is expressed by the bending energy which depends on the magnitude of the bending constants [92].

Single-chain nonionic surfactants, such as the C_iE_j surfactants considered here, have low bending constants (< 1 kT) [93,112] leading to flexible microemulsions [113]. Moreover, at the fish-tail-temperature T* and for a WOR (v/v) equal to one, the C_iE_j/Oil/Water systems are at the zero spontaneous curvature (H = H_0 = 0) [23]. The evolution of the fish-tail-temperature T* according to the EACN of the oil and the PACN of the surfactant can thus be rationalized in terms of the spontaneous packing parameter $\overline{P_0}$. This parameter is an extension for SOW ternary systems of the spontaneous "packing parameter" P_0 of a surfactant introduced by Israelachvili *et al.* in 1976 for SW binary systems [114]. P_0 is a dimensionless number defined as $v_{surf}/(a_{surf}.l_{surf}$ where v_{surf} is the volume of the surfactant tail and l_{surf} is the length of the tail averaged over all conformations [23]. For alkyl chains, this length is about 80-90 % of

the extended chain length [115]. The area a_{surf} per surfactant molecule is the area that minimizes free energy. P_0 mainly depends on the chemical structure of the surfactant but also on variables such as temperature and electrolytes (nature and concentration) that modify the size, i.e. the hydration, of the hydrophilic head. The shape of the aggregates spontaneously formed in water by the surfactant above the CMC is governed by its P_0 value [116].

For SOW systems, the interaction of the oil with the interfacial surfactant monolayer influences the packing parameter of the surfactant. In particular, the expression of the packing parameter must take into account the "penetrating oil" within the interfacial surfactant monolayer. In order to rationalize the behaviour of such systems, Tchakalova *et al.* developed the Constant Interfacial Thickness model (CIT) [37]. This model takes into account the changes induced by the oil on the values of *v* and *a*. The sole hypothesis is relative to the thickness of the hydrophobic layer, which is assumed to remain constant and equal to the length of the surfactant tail l_{surf}. The penetration of the oil leads to the formation of a mixed (surfactant/oil) interfacial monolayer, so the area and the volume per surfactant molecule increase. Therefore, for ternary systems, Tchakalova *et al.* introduced the "effective packing parameter" $\overline{P_{eff}}$ which takes into account the entire physicochemical environment of the surfactant (Eq. 15) [38].

$$\overline{P_{eff}} = \frac{v_{surf} + \tau v_{oil}}{(a_{surf} + \tau a_{oil})l_{surf}} \qquad (15)$$

where:

- v_{surf} and l_{surf} are the volume and the length of the surfactant tail,
- a_{surf} is the equilibrium area per surfactant molecule within the interfacial film,
- v_{oil} is the molecular volume of the oil,
- a_{oil} is the area occupied by each oil molecule located at the oil/water interface
- $\tau = N_{oil}/N_{surf}$ is the ratio between the number of oil molecules and the number of surfactant molecules at the interface.

$\overline{P_{eff}}$ can be measured by scattering of radiation (DLS [37], SAXS [117] or SANS [118]), provided that the Porod limit is measurable and the surfactant present as monomer in water or oil is negligible. It may be equal to the spontaneous packing parameter $\overline{P_0}$. or not [119]. Nevertheless, at the fish-tail temperature T*, the effective (H) and the spontaneous (H_0) curvatures are both equal to zero and $\overline{P_{eff}} = \overline{P_0} = 1$ [23]. Depending on its affinity for the interfacial film, the oil penetrates more or less deeply within the interfacial surfactant monolayer. The higher the polarity of the oil (the lower the EACN), the stronger the affinity

for the interfacial film and the higher is τ. As the value of a_{oil} of oils is much smaller than a_{surf}, the penetration of the oil mainly increases the numerator of equation 15.

To illustrate this behavior, let us first consider an optimum microemulsion system at T* having an interfacial film with zero mean curvature and an effective packing parameter $\overline{P_{eff}}$ equal to 1 (Figure 13 middle). Increasing the polarity of the oil favors its penetration into the surfactant monolayer and its localization closer to the W/O interface leading to an increase of $\overline{P_{eff}}$ as schematically represented in Figure 13 left. In contrast, a decrease in temperature favors the hydration of the polar heads of C_iE_j surfactants by water molecules which dramatically increases a_{surf}. (Figure 13 right). As a consequence, the lower the EACN of an oil, i.e. the higher its polarity, the deeper it penetrates into the interfacial film and the lower will be the optimum temperature T* required to restore a balanced system with $\overline{P_{eff}} = 1$.
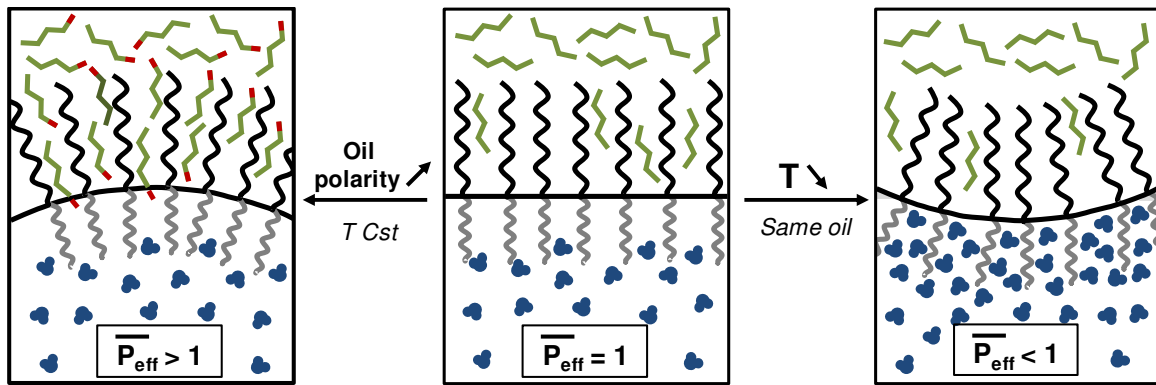
Figure 13. Influence of oil polarity and temperature on the curvature of the interfacial film of a C_iE_j/Oil/Water microemulsion system. Middle: Well-balanced system with WOR = 1 and zero curvature where H = H$_0$ = 0 and $\overline{P_{eff}} = \overline{P_0} = 1$. Left: Effect of penetrating polar oil where the red head symbolizes the polar function. Right: Effect of decreasing temperature (redrawn from [36]).

It is well admitted that all oils are prone to penetrate more or less into the surfactant palisade layer. Thus, Requena *et al.* [120] and Chen *et al.* [121] showed that *n*-alkanes shorter than the surfactant tail penetrate the interfacial layer and increase the effective volume of the surfactant tail ($v_{surf} + \tau v_{oil}$). The restriction about the maximum length of the penetrating alkane is somewhat questionable, as Queste *et al.* demonstrated that the linearity between T* and ACN is maintained even when the ACN is twice the number of carbons of the hydrophobic tail of the surfactant [31]. For polar oils, the behaviour is more complex because such oils exhibit very different degrees of penetration, as shown by Kanei *et al.* by studying the penetration of fragrance within liquid crystal of $C_{12}E_8$ [78]. They showed that fragrant molecules exhibit different behaviours varying from an oil-like for terpenes localized in the hydrocarbon core of the surfactant assembly to a co-surfactant-like for terpenic alcohols

localized within the surfactant palisade layer. In the same way, Tchakalova *et al.* showed that fragrances always increase $\overline{P_{eff}}$ [37]. However, we consider in this review only true ternary systems whereas Tchakalova *et al.* added a fourth compound to fixed ternary mixtures $C_{10}E_5$/n-decane/water or $C_{10}E_5$/*i*-Pr myristate/water. By measuring changes in fish-diagrams by the addition of a wide range of perfumery raw materials, they could classify them according to their interfacial affinity: alcohols > aldehydes > terpenes > aromatics [76]. However, this method does not provide reliable EACN values for oils because the rule of ideal mixing of oils does not hold as discussed above.

8 Quantitative Structure-Property Relationship (QSPR) modelling of EACNs with COSMO-RS descriptors

Currently, available experimental data do not permit the calculation of the characteristic values of the oils v_{oil}, a_{oil} and τ appearing in equation 6. However, knowledge of the chemical structure of the oils and their EACNs is sufficient to infer general trends in the ability of a particular functional group to penetrate the interfacial film and it is even possible to predict the EACN values of unknown oils using QSPR (Quantitative Structure-Property Relationship) approaches coupled with suitable molecular descriptors. Actually, the experimental determination of the EACN of new oil is time-consuming and requires significant amounts of costly monodisperse-C_iE_j surfactants. It is therefore tempting to perform a chemometric treatment of the available EACNs by QSPR to predict EACNs of new oils including virtual oils not yet synthesized.

8.1 QSPR Analysis of physicochemical properties

The QSPR analysis assumes that a measurable property such as the EACN an oil is correlated with its chemical structure. Therefore, this property could be modelled from known EACNs using appropriate molecular descriptors. Such a model could then be used to predict EACNs of unknown oils. This approach has been implemented with success to predict EACNs of hydrocarbons (alkanes, alkenes, alkynes, aromatics) for which the area occupied by each oil molecule a_{oil} (Eq. 15) is expected to be small [35]. It has also been used to predict, more crudely, EACN values for polar oils (esters, ketones, acetates, nitriles) that exhibit more complex interfacial behaviour because a_{oil} is no longer negligible [36].

The key step in a QSPR analysis is the generation of relevant molecular descriptors capable of modelling the property under study with a small number of 2D or 3D descriptors:

- 2D descriptors are calculated from purely atomic and connectivity properties, for instance, molecular weight, molecular branching and sum of atomic polarizabilities.

- 3D descriptors use atomic coordinates. Some examples are volume, dipole moment, molecular surface area, donor surface area and hydrophobic surface area.

Once a number of descriptors are calculated, they are sent to a model builder which performs multiple linear regressions on all the descriptors in order to generate a fitted model. This model is then evaluated for its significance and validity. If the model evaluator indicates that the model should be rejected, it is re-calculated with new descriptors until a satisfactory model is found. Thereby, Bouton *et al.* have-established a QSPR model to predict the EACNs of hydrocarbons oils with the modelling software Molecular Operating-Environment (MOE) [33]. MOE can calculate hundreds of descriptors for a single molecule, including some physical properties, topological indices and structural keys. Among this huge number of descriptors, only two were required, namely *"Average negative softness"* and *"Kier A3"* to build a robust linear model able to effectively predict the EACN values of 43 different hydrocarbons (Eq. 16)

$$EACN_{calc} = 2.88 \times (Average\ negative\ softness) + 0.88 \times (Kier\ A3) - 19.84 \quad (16)$$

Unfortunately, these two descriptors have no clear structural or physicochemical meaning. In order to get a deeper insight into the molecular factors influencing the EACN of oils and to get a sound and predictive model, more meaningful descriptors derived from the COSMO-RS theory were used later.

8.2 COSMO-RS σ-Moments as relevant molecular descriptors

The COSMO-RS theory (Conductorlike Screening MOdel for Real Solvents), introduced by Klamt in 1995, is based on unimolecular quantum chemical calculations combined with statistical thermodynamics [122]. This model, which is implemented in the COSMOtherm software, provides the necessary information for computing the chemical potential μ of a solute in a liquid phase without requiring any experimental input. This chemical potential can then be transformed into relevant physicochemical properties such as the partition coefficient of compounds between two phases [123] or between an aqueous phase and a micelle [124]. Therefore, for a SOW system, COSMOtherm should be able to calculate the amount of a given oil penetrating into the interfacial film of surfactant considered here as a pseudo-phase. However, the chemical potential μ of the oil inside the interfacial film cannot be directly calculated because the standard version of COSMOtherm is able to describe bulk liquid

phases and not self-organized surfactant films [125]. For such complex systems, an alternative approach based on descriptors called COSMO-RS σ-moments, enables an indirect treatment. Starting from the 2D molecular structure of the oil X, COSMOtherm generates the so-called 3D σ-surface, a slightly inflated Van der Waals surface of X. The full 3D information about the charge density repartition on the σ-surface is then converted into a curve $p^X(\sigma)$, i.e. the σ-profile of the molecule X, which is a smoothed histogram expressing how much of the σ-surface lies in the polarity interval [σ − dσ/2, σ + dσ/2] [36]. Figure 14 shows as examples the σ-surface and the σ-profiles of three C12 oils namely, dihexylether, dodecanenitrile and 2-dodecanone.
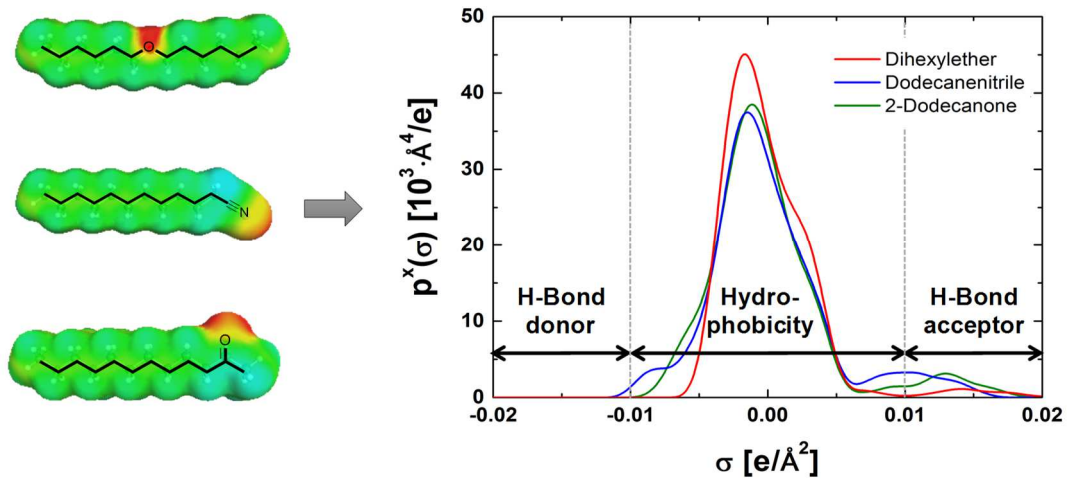
Figure 14. Conversion with COSMOtherm of the 2D molecular structure of three oils, namely dihexylether (red), dodecanenitrile (blue) and 2-dodecanone (green) into their 3D σ-surfaces (left) and then into their σ-profiles (right). Redrawn from [36].

As shown by Klamt, the logarithmic partition coefficient K of a solute X between two phases can be represented as a linear combination of its so-called σ-moments M_i^X according to Eq 17 [126]

$$RTlnK = c_{acc}M_{acc}^X + c_{don}M_{don}^X + \sum_{i=0}^m c_i M_i^X \qquad (17)$$

The σ-moments M_i^X are calculated from the σ-profiles $p^X(\sigma)$ of the studied compound X, according to equations 18-20.

$$M_{acc}^X = \int_{+\sigma_{hb}}^{+\infty} p^X(\sigma)\,(\sigma - \sigma_{hb})d\sigma \qquad (18)$$

$$M_{don}^X = \int_{-\infty}^{-\sigma_{hb}} p^X(\sigma)\,(-\sigma - \sigma_{hb})d\sigma \qquad (19)$$

$$M_i^X = \int_{-\infty}^{-\infty} p^X(\sigma)\,\sigma^i d\sigma \qquad (20)$$

The two "hydrogen-bonding" σ-moments M_{acc}^X (Eq 18) and M_{don}^X (Eq 19) express the ability of X to interact as a hydrogen-bond acceptor and donor, respectively. They have a non-zero value only when the σ-profile of X exceeds the range $[-\sigma_{hb}, +\sigma_{hb}]$, where σ_{hb} is an appropriate value of the hydrogen-bond cutoff equal to 0.01 e.Å^{-2}. For instance, the three oils shown in Fig. 14 exhibit a significant electron-donor ability expressed in the σ-profile as small peaks between 0.01 and 0.02 e.Å^{-2}. In contrast they do not have any significant electron-acceptor ability (no peak below -0.01 e.Å^{-2}).

The remaining σ-moments are obtained from the σ-profile $p^X(\sigma)$ according to Eq 20. Usually a mere development of the series up to m = 6 is sufficient to adequately model the partition coefficient K (Eq. 17). The first σ-moments M_i^X have a clear physical meaning. The zero-order moment M_0^X is equal to the total molecular surface area of the solute X. The first-order moment M_1^X is the total polarization charge on the σ-surface of X and is equal to zero for uncharged compounds such as all the oils considered in this paper. The second-order moment M_2^X expresses the polarity of X. The third-order moment M_3^X is a measure of the asymmetry of the σ-profile. Higher σ-moments possess only a mathematical interpretation.

8.3   Modelling EACNs of hydrocarbon oils

According to the expression (15) of the effective packing parameter $\overline{P_{eff}}$, the EACN of an oil is related to its molecular volume (v_{oil}) and to its affinity for the interfacial film (τ). In particular, polar oils have a stronger affinity than hydrocarbons for the interfacial film and tend to position their polar function near the O/W interface or even within the hydrated PEO zone (Fig. 13). As a result, they have a high partition coefficient τ and, unlike hydrocarbons, they significantly modify the denominator of $\overline{P_{eff}}$ through the parameter a_{oil}. Likewise, the monomolecular solubility of the surfactants C_iE_j in the oil phase is substantially higher in polar oils than in hydrocarbons. In summary, the EACN of an oil depends in a complex way on its partition coefficient between the surfactant layer and the oil phase as well as the average position of the oil molecules into this film [127]. Since the logarithmic partition coefficient K of a solute X between two phases can be written as a linear combination its σ-moments (Eq. 17), the nine σ-moments (M_{acc}^X, M_{don}^X, M_0^X and M_i^X with i = 2−6) are expected to be effective descriptors for a QSPR analysis of EACN values.

At first, such a regression analysis has been performed to model the EACNs of 62 highly diverse liquid hydrocarbons including (cyclo)alkanes, (cyclo)alkenes, terpenes, aromatics, alkynes, and chloroalkanes [35]. Experimental EACNs were the dependent variables and the

σ-moments the independent variables. The significance of each parameter was then verified according to the t-test in order to delate the most insignificant descriptors. Consequently, seven uninformative σ-moments were eliminated leading to a predictive model that involves only the two descriptors M_0^{oil} (surface area of the molecule) and M_2^{oil} (polarity of the oil) reported in Eq. 21.

$$EACN_{pred}^{oil} = -4.03 + 0.07 \times M_0^{oil} - 0.33 \times M_2^{oil} \qquad (21)$$

The linear correlation between predicted EACNs and experimental values shows an excellent coefficient of determination (R^2 = 0.98) and a small standard error of the estimate (SEE = 0.82). Moreover, this QSPR model sheds some light on the structural parameters influencing EACNs. Actually, 9 oils having the same number of carbon atoms (C_{10}) were selected and positioned in Figure 15 as a function of their molecular surface M_0^{oil} (X-axis) and their polarity M_2^{oil} (Y-axis). The four inclined straight lines correspond to the iso-EACN curves calculated from Eq. 21. n-Decane is used as a reference oil for identifying oils having a smaller or larger molecular area, depending on whether they are located to the left or right of the dotted vertical line. Here, all selected cyclic oils have a much smaller molecular surface than decane. The dashed horizontal line separates, in turn, saturated cycloalkanes from unsaturated oils that are significantly more polar than n-decane.
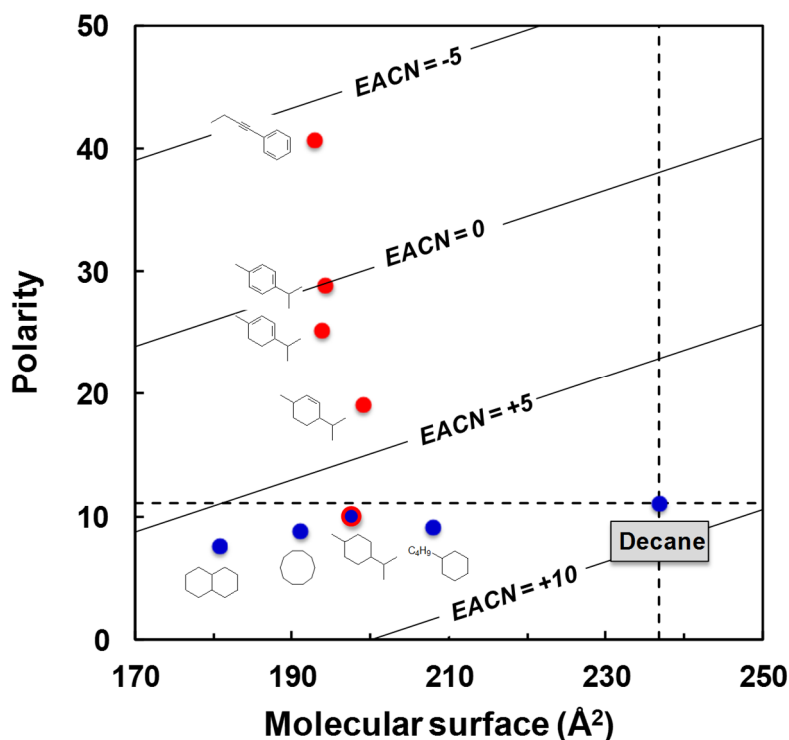
Figure 15. Position of a selection of C10 oils as a function of their molecular surface (M_0^{oil}) and their polarity (M_2^{oil}). Inclined straight lines correspond to the iso-EACN curves calculated from eq 21. Red dots: Influence of

the polarity on the EACN value, Blue dots: Influence of the molecular surface on the EACN value. Data from [35].

Comparing experimental EACNs of alkanes and cycloalkanes in Figure 15, one notes that they vary substantially from 5.3 (cis-decalin) to 10.0 (n-decane) while they have approximately the same polarity (M_2^{oil}) as n-decane. Thus, the relatively low EACN values of cyclic oils do not result from their greater polarity but from their smaller molecular surface which decreases their interactions with surrounding oil molecules and increases their partition coefficient toward the interfacial film of surfactants. In the same way, it is worth comparing the EACN of p-menthane (blue-red dot) with that of the three unsaturated and aromatic derivatives (p-menth-2-ene, α-terpinene, and p-cymene) located above it in Figure 15. Actually, these five molecules have almost identical surfaces but differ markedly with regard to their polarity as well as their EACN that follow the same trend starting from p-menthane (EACN = + 6.0) to p-cymene (EACN = − 0.4). To summarize, the more the oil is polar, the lower is its EACN in the following order: alkanes < alkenes < dienes < aromatics < alkynes.

8.4 Modelling EACNs of polar oils

The same approach was extended to functionalized oils by Lukowicz et al. [36] in order to build a more general predictive model, suitable for both polar oils and hydrocarbons. Therefore, they performed a multilinear regression analysis starting from the experimental EACN values of 70 polar (alkene, ether, ester, ketone, nitrile and chloroalkene) and apolar (hydrocarbons) oils and their 8 σ-moments. They found a satisfactory model involving only the three descriptors M_0^{oil}, M_2^{oil} and M_{acc}^{oil}, (Eq. 22) that provides a fair linear correlation between experimental and predicted EACNs with $R^2 = 0.92$ and SEE = 1.1.

$$EACN_{pred}^{oil} = -4.85 + 0.06 \times M_0^{oil} - [0.23 \times M_2^{oil} - 0.33 \times M_{acc}^{oil}] \qquad (22)$$

Eq. 22 can be separated in two parts, on the one hand, the contribution of the molecular surface (M_0^{oil}) and, on the other hand, the cumulated contribution of the polarity (M_2^{oil}) and the hydrogen-bond-accepting ability of the molecule (M_{acc}^{oil}) which expresses the overall affinity of the molecule for the polar zone of the interfacial film.
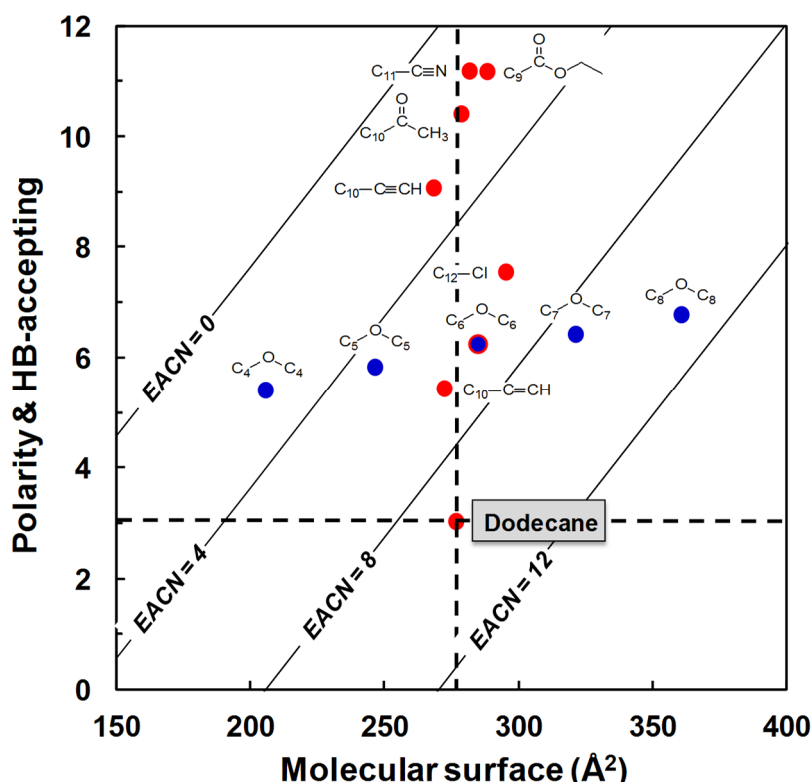
Figure 16. Red dots: Influence of the polar functions on the EACN of C12-oils. Blue dots: Influence of increasing carbon number on the EACN of homologous dialkylethers. The inclined iso-EACN curves are calculated according to Eq. (17). Data from [36].

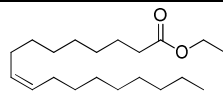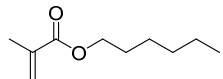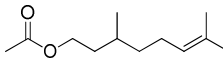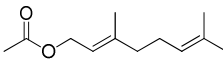*Molecular interpretation of the factors influencing EACNs of polar oils*

In Section 6.3, it was shown that the linear evolutions of the EACNs of dialkylethers, ethyl alkanoates, alkanenitriles and 2-alkanones with the carbon number are not parallel to the straight line of n-alkanes. It is striking that only the most polar series of oils containing nitrogen or oxygen atoms exhibit this peculiar behaviour in contrast to the less polar oils (hydrocarbons and 1-chloroalkanes). Looking at the M_{acc}^{oil} values, it can be seen that these polar molecules have a significant hydrogen-bond-acceptor capability in contrast to other molecules [36,104]. It reflects their relatively strong affinity for the polar zone of the interfacial film due to the favourable interactions with the hydrated polyethoxylated chain. More precisely, when M_{acc}^{oil} value is higher than 3, the chemical function is so hydrophilic that it strives to remain in contact with the hydrated region of the surfactants palisade even when the hydrophobic chain is relatively long. Therefore, the penetration ratio τ is decreasing less steeply with increasing carbon number compared to less polar oils. This positioning is facilitated when the hydrophilic function is located at the chain end as in the case of nitriles. In other words, these oils behave as HB-acceptor co-surfactants contrasting with alcohols which are HB-donor co-surfactants. Nevertheless, when the polar chemical function is not

located at the chain end as in the case of ketones and symmetrical dialkylethers, the positioning of the hydrophilic function in the hydrated zone of the palisade is impeded and the co-surfactant effect is weakened. Based on these considerations, it is not surprising that the model requires the three physicochemical descriptors M_0^{oil}, M_2^{oil} and M_{acc}^{oil}.

EACNs of polyfunctional oils

Since many valuable oils, such as fragrances or polymerizable monomers, have several chemical functions, it is worth to examine whether Eq. 22 is also able to predict the EACNs of selected polyfunctional oils included in Table 7.

Table 7. Experimental EACNs of selected polyfunctional oils compared with the predicted EACNs calculated with Eq. 22 involving three σ-moments of the oils.

Polyfunctional oil		M_0^{oil}	M_2^{oil}	M_{acc}^{oil}	$EACN_{pred}^{oil}$	$EACN_{exp}^{oil}$
Ethyl oleate		446.5	70.5	5.1	+ 8.0	+ 7.2
Hexyl methacrylate		242.0	49.6	4.4	+ 0.0	+ 0.1
Citronellyl acetate		263.1	62.3	5.4	- 1.3	- 0.2
Geranyl acetate		267.6	69.4	4.8	-2.9	- 0.6

Actually, Eq. 22 correctly predicts the EACNs of (i) ethyl oleate studied by Kahlweit et al. [108] as well as hexylmethacrylate studied in details by Strey et al. [81] for the design of polymerizable microemulsions. Looking at the two terpenic acetates, it appears that citronellyl acetate is fairly well predicted whereas, for geranyl acetate, the predicted value (−2.9) is significantly below the experimental value (−0.6). This discrepancy can be explained by the method used to calculate the "polarity" descriptor M_2^{oil}. Actually, M_2^{oil} considers all functional groups of the molecules, no matter where they are within the molecular structure. In this specific case, it can be assumed that the acetate functional group is located close to the interface, while the double bonds of geranyl acetate are forced to stay in the hydrophobic bulk of the interfacial film. Consequently, the calculated M_2^{oil} overestimates the "effective" polarity of the oil. As a consequence, the predicted EACN value is significantly lower (ΔEACN = -2.3) than the experimental one. On the other hand, the experimental EACN of

citronellyl acetate with a single double bond is only slightly lower (ΔEACN = -1.1) than the experimental one. Hence, the model is able to satisfactorily predict the EACN of polyfunctional oils. However, when their functional groups are distributed throughout the molecular structure, the model tends to overestimate the contribution of the polar part and thus predicts too low EACNs. To get a better prediction of their EACN it must be known, which part of the compound is located directly at the interface and subtract manually the contribution of other polar groups from M_2^{oil}.

Actually, just looking at the influence of structural and functional features on the relevant σ-moments M_0^{oil}, M_2^{oil} and M_{acc}^{oil}, one can infer the main parameters influencing the EACN of polar oils. Eq. 22 includes two main contributions, namely the size of the molecule (M_0^{oil}) and its polarity/HB-accepting-ability [$0.23 M_2^{oil} + 0.33 M_{acc}^{oil}$]) which are represented graphically in Fig. 16. Two families of oils are positioned in this graph, a homologous series of dialkylethers appears as blue dots while a series of C_{12}-oils, with different functions are shown as red dots. The inclined straight lines correspond to the iso-EACN curves calculated from Eq. 22. n-Dodecane is used as a reference oil, to highlight the effect of polar groups on EACN values. All compounds indicated in red have approximatively the same molecular surface area. However, their EACNs drastically fall when their polarity/HB-accepting-ability contribution increases. According to this graphical representation, 1-nitriles, 2-alkanones and ethyl alkanoates appear to be the most polar oils, followed by 1-alkynes and finally the much less polar oils 1-chloroalkane, dialkylether, 1-alkene and n-alkane. Slight deviations in the order as compared to Table 5 can be attributed to the SEE ($\pm$1.1) of the predicted values. On the other hand, following up the evolution of the experimental EACNs of homologous dialkyethers with increasing carbon number shows that the wide variation of EACN values from 3.0 (dibutylether) to 10.3 (dioctylether) is solely due the large difference in their molecular surfaces (M_0^{oil}) since all these oils have approximately the same polarity/HB-accepting-ability. Note that n-alkanes are not very well predicted by Eq. 22, since they were not considered in the training set. Actually M_0^{oil} alone would be sufficient for a perfect correlation between experimental and predicted EACNs for these non-polar oils.

9 Conclusions and future prospects

The notions of PACN (under the names of EPACNUS and N_{min}) and EACN were coined in the 70s to quantify the lipophilic-hydrophilic tendency of surfactants and the hydrophobicity of oils by comparing it to a series of *n*-alkanes whose number of carbons (ACN) are used as

reference. [24,128]. Unfortunately, most of the EACN values published since then are approximate because they were determined with complex SOW systems based on four or five ingredients including ill-defined surfactants.

Here, we show that the Fish-Tail-Method (FTM) can provide accurate and unambiguous PACN and EACN values. It is based on the detection of the fish-tail-temperature T* of the fish diagrams of well-defined C_iE_j/Oil/Water ternary systems [31]. Experimental values of T* are then analyzed on the basis of a normalized version of the HLD equation denoted HLD_N (Eq. 4) [58]. This equation includes only three meaningful parameters, namely the EACN (Equivalent-ACN) of the oil, the PACN (Preferred-ACN) of the surfactant and the τ parameter that reflects its sensitivity towards temperature. This simplified expression of the HLD equation offers the advantage of giving a simple and intuitive physical meaning to the non-zero values of HLD_N. Actually, an increase of one HLD_N unit corresponds to a physicochemical modification of the SOW system similar to that provided by removing one CH_2 group to an n-alkane oil. Moreover, HLD_N is, to within a constant, proportional to the mean curvature H of the interfacial film over a wide temperature range around the optimum temperature T*

A systematic analysis of the fish diagrams of C_iE_j/n-Alkane/Water systems, carefully built by Kahlweit's, Strey's and Sottmann's research groups graphically shows that T* varies linearly with the length of n-alkane oils. These bundles of straight lines are then used as baseline to assign reliable EACN values to a wide range of oils corresponding to real or virtual n-alkanes having the same T* values. These calibration lines are also used to accurately estimate the amphiphilicity of C_iE_j surfactants through their PACN that corresponds to the number of carbon atoms of the n-alkane (or a mixture of n-alkane) which provides an optimum formulation at 25 °C in the absence of salt and co-surfactant. It is shown that PACNs of C_iE_j surfactants (i $\geq$ 8) are linearly correlated to their cloud points (R^2 = 0.99), to the "Characteristic curvature" Cc (R^2 = 0.97), to Griffin's HLBs (R^2 = 0.90) and to the PIT-slope values (R^2 = 0.92). It should be noted that, according to the definition of HLD_N, the PACN of a surfactant varies inversely with its HLB. The more hydrophilic a surfactant, the lower its PACN, or even negative. In particular, only surfactants having a PACN lower than 15 are water-soluble at room temperature.

The EACNs of oils and the PACNs of surfactants have been rationalized in terms of the "effective packing parameter" of the interfacial film which mainly depends on the chemical

structure of the surfactant and the ability of oil molecules to penetrate more or less deeply into the surfactant layer [38]. QSPR modelling of EACNs values using descriptors derived from the COSMO-RS theory provides clarity regarding the molecular criteria influencing the spontaneous curvature of the interfacial film. For hydrocarbon oils (alkanes, alkenes, terpenes, alkynes, aromatics) the volume and the polarity of the oil molecule are sufficient to predict with an excellent precision (R^2 = 0.98) experimental values of EACNs [35]. However, for functionalized oils (ethers, esters, ketones, nitriles), the QSPR model is less accurate (R^2 = 0.92) and requires one additional descriptor, namely the electron-donor ability of the molecule [36]. In summary, the ability of an oil to penetrate the interfacial film and to decrease the EACN value is in the following order: 2-ketones > 1-nitriles > ethyl alkanoates ≈ 1-alkynes ≈ n-alkylbenzenes > 1-chloroalkanes ≈ dialkylethers > 1-alkenes > *n*-alkylcyclohexanes > *i*-alkanes > *n*-alkanes.

The interpretation of the EACN parameter based on the ability of oil molecules to penetrate the interfacial film raises the question of the universality of the EACN values when the structure of the surfactant used to establish the calibration lines is changed. When the interfacial film is composed of ethoxylated surfactants, it is likely that the oxygen functions of polar oils penetrate somewhat within the hydrated polyethoxylated head groups. Therefore, if the C_iE_j surfactants are replaced by ionic surfactants such as SDS [129] or dialkyl sodium sulfosuccinate [130,131] the penetration is expected to be less important within the polar heads and that the measured EACN would be higher than that determined with C_iE_j surfactants.

It should be noted that the fish-tail-method based on the C_iE_j/Oil/Water ternary systems is generally not applicable to determine the EACN of hydrogen-bond-donating oils (alcohols, phenols, amines, amides and carboxylic acids) as well as the PACN of lipophilic (HLB < 10) or highly hydrophilic (HLB > 15) surfactants. To evaluate the PACN values of such amphiphiles, it is better to resort to the more versatile PIT-slope-method which is based on the perturbation, provided by the oil or the surfactant under study, to the phase inversion temperature of a reference system $C_{10}E_4$/ *n*-Octane/Water [60,132].

Until very recently, no theoretical model was able to calculate, without adjustable parameters, the C_iE_j/Oil/Water ternary phase diagrams. However, the recent release of the COSMOplex program should change the situation since it can calculate, from the sole molecular structures

of the surfactant and the oil, the equilibria of self-organizing systems based on surfactants and to predict the spontaneous formation of Winsor III systems [125].

Hopefully, the description of an unambiguous method for determining EACNs and PACNs and the compilation of all reliable EACN values of well-defined oils will contribute to popularize these useful parameters and help formulation scientists to design more quickly micro- and macro-emulsions with pre-established morphologies and properties [21,76,80,133,134].

Acknowledgement

10   References

[1] Aubry JM, Schorsch G. Formulation - Présentation générale. Tech Ing, Genie Procedes 1999:J2110/1-J2110/20.

[2] Bancroft WD. The theory of emulsification, V. J Phys Chem 1913;17:501–519.

[3] Bancroft WD. The theory of emulsification, VI. J Phys Chem 1915;19:275–309.

[4] Griffin WC. Classification of surface-active agents by" HLB". J Soc Cosmet Chem 1949;1:311–326.

[5] Griffin WC. Calculation of HLB Values of Non-ionic Surfactants. J Soc Cosmet Chem 1954;5:249–56.

[6] Becher P. Hydrophile-Lipophile Balance: History and Recent Developments. J Dispersion Sci Technol 1984;5:81–96. https://doi.org/10.1080/01932698408943210.

[7] Winsor PA. Solvent properties of amphiphilic compounds. Butterworths Scientific Publications; 1954.

[8] Winsor PA. Binary and multicomponent solutions of amphiphilic compounds. Solubilization and the formation, structure, and theoretical significance of liquid crystalline solutions. Chem Rev 1968;68:1–40. https://doi.org/10.1021/cr60251a001.

[9] De Gennes PG, Taupin C. Microemulsions and the flexibility of oil/water interfaces. J Phys Chem 1982;86:2294–304. https://doi.org/10.1021/j100210a011.

[10]   Wennerström H, Balogh J, Olsson U. Interfacial tensions in microemulsions. Colloids Surf, A 2006;291:69–77. https://doi.org/10.1016/j.colsurfa.2006.09.027.

[11]   Salager JL, Loaiza-Maldonado I, Minana-Perez M, Silva F. Surfactant-oil-water systems near the affinity inversion. Part I: Relationship between equilibrium phase behavior and emulsion type and stability. J Dispersion Sci Technol 1982;3:279–92. https://doi.org/10.1080/01932698208943642.

[12]   Bourrel M, Graciaa A, Schechter RS, Wade WH. The relation of emulsion stability to phase behavior and interfacial tension of surfactant systems. J Colloid Interface Sci 1979;72:161–3. https://doi.org/10.1016/0021-9797(79)90198-X.

[13]   Salager JL, Minana-Perez M, Anderez JM, Grosso JL, Rojas CI, Layrisse I. Surfactant-oil-water systems near the affinity inversion. Part II: Viscosity of emulsified systems. J Dispersion Sci Technol 1983;4:161–73. https://doi.org/10.1080/01932698308943361.

[14]   Sottmann T, Strey R. Ultralow interfacial tensions in water-n-alkane-surfactant systems. J Chem Phys 1997;106:8606–15. https://doi.org/10.1063/1.473916.

[15]   Pizzino A, Molinier V, Catte M, Ontiveros JF, Salager J-L, Aubry J-M. Relationship between Phase Behavior and Emulsion Inversion for a Well-Defined Surfactant (C10E4)/n-Octane/Water Ternary System at Different Temperatures and Water/Oil Ratios. Ind Eng Chem Res 2013;52:4527–38. https://doi.org/10.1021/ie302772u.

[16]   Shinoda K, Arai H. The correlation between phase inversion temperature in emulsion and cloud point in solution of nonionic emulsifier. J Phys Chem 1964;68:3485–90.

[17]   Salager JL, Morgan JC, Schechter RS, Wade WH, Vasquez E. Optimum Formulation of Surfactant/Water/Oil Systems for Minimum Interfacial Tension or Phase Behavior. Soc Pet Eng J 1979;19:107–15. https://doi.org/10.2118/7054-PA.

[18]   Salager J-L, Marquez N, Graciaa A, Lachaise Jean. Partitioning of Ethoxylated Octylphenol Surfactants in Microemulsion-Oil-Water Systems: Influence of Temperature and Relation between Partitioning Coefficient and Physicochemical Formulation. Langmuir 2000;16:5534–9. https://doi.org/10.1021/la9905517.

[19]   Salager J-L, Antón RE, Anderez JM, Aubry J-M. Formulation des microémulsions par la méthode du HLD. Tech Ing, Genie Procedes 2001:J2-157/1-J2-157/20.

[20]   Salager J-L, Anton R, Aubry J-M. Formulation des émulsions par la méthode du HLD. Tech Ing, Genie Procedes 2006;41:J2158/1-J2158/17.

[21]   Salager J-L, Anton RE, Sabatini DA, Harwell JH, Acosta EJ, Tolosa LI. Enhancing solubilization in microemulsions - State of the art and current trends. J Surfactants Deterg 2005;8:3–21. https://doi.org/10.1007/s11743-005-0328-4.

[22]   Acosta E, Szekeres E, Sabatini DA, Harwell JH. Net-Average Curvature Model for Solubilization and Supersolubilization in Surfactant Microemulsions. Langmuir 2003;19:186–95. https://doi.org/10.1021/la026168a.

[23]   Kunz W, Testard F, Zemb T. Correspondence between Curvature, Packing Parameter, and Hydrophilic–Lipophilic Deviation Scales around the Phase-Inversion Temperature. Langmuir 2009;25:112–5. https://doi.org/10.1021/la8028879.

[24]   Cayias JL, Schechter RS, Wade WH. Modeling Crude Oils for Low Interfacial Tension. Soc Pet Eng J 1976;16:351–7. https://doi.org/10.2118/5813-PA.

[25]   Cash L, Cayias JL, Fournier G, Macallister D, Schares T, Schechter RS, et al. The application of low interfacial tension scaling rules to binary hydrocarbon mixtures. J Colloid Interface Sci 1977;59:39–44. https://doi.org/10.1016/0021-9797(77)90336-8.

[26]   Nardello V, Chailloux N, Poprawski J, Salager J-L, Aubry J-M. HLD concept as a tool for the characterization of cosmetic hydrocarbon oils. Polym Int 2003;52:602–9. https://doi.org/10.1002/pi.1012.

[27]   Poprawski J, Catte M, Marquez L, Marti M-J, Salager J-L, Aubry J-M. Application of hydrophilic-lipophilic deviation formulation concept to microemulsions containing pine oil and nonionic surfactant. Polym Int 2003;52:629–32. https://doi.org/10.1002/pi.1030.

[28]   Graciaa A, Lachaise J, Cucuphat C, Bourrel M, Salager JL. Interfacial segregation of an ethyl oleate/hexadecane oil mixture in microemulsion systems. Langmuir 1993;9:1473–8. https://doi.org/10.1021/la00030a008.

[29]   Szekeres E, Acosta E, Sabatini DA, Harwell JH. Preferential solubilization of dodecanol from dodecanol–limonene binary oil mixture in sodium dihexyl sulfosuccinate microemulsions: Effect on optimum salinity and oil solubilization capacity. J Colloid Interface Sci 2005;287:273–87. https://doi.org/10.1016/j.jcis.2005.01.092.

[30]   Bouton F, Durand M, Nardello-Rataj V, Serry M, Aubry J-M. Classification of terpene oils using the fish diagrams and the Equivalent Alkane Carbon (EACN) scale. Colloids Surf, A 2009;338:142–7. https://doi.org/10.1016/j.colsurfa.2008.05.027.

[31]   Queste S, Salager JL, Strey R, Aubry JM. The EACN scale for oil classification revisited thanks to fish diagrams. J Colloid Interface Sci 2007;312:98–107. https://doi.org/10.1016/j.jcis.2006.07.004.

[32]   Engelskirchen S, Elsner N, Sottmann T, Strey R. Triacylglycerol microemulsions stabilized by alkyl ethoxylate surfactants-A basic study; Phase behavior, interfacial tension and microstructure. J Colloid Interface Sci 2007;312:114–21. https://doi.org/10.1016/j.jcis.2006.09.022.

[33]   Bouton F, Durand M, Nardello-Rataj V, Borosy AP, Quellet C, Aubry J-M. A QSPR Model for the Prediction of the "Fish-Tail" Temperature of CiE4/Water/Polar Hydrocarbon Oil Systems. Langmuir 2010;26:7962–70. https://doi.org/10.1021/la904836m.

[34]   Ontiveros JF, Pierlot C, Molinier V, Pizzino A, Salager J-L, Aubry J-M. Classification of ester oils according to their Equivalent Alkane Carbon Number (EACN) and asymmetry of fish diagrams of C10E4/ester oil/water systems. J Colloid Interface Sci 2013;403:67–76. https://doi.org/10.1016/j.jcis.2013.03.071.

[35]   Lukowicz T, Benazzouz A, Nardello-Rataj V, Aubry J-M. Rationalization and Prediction of the Equivalent Alkane Carbon Number (EACN) of Polar Hydrocarbon Oils with COSMO-RS σ-Moments. Langmuir 2015;31:11220–6. https://doi.org/10.1021/acs.langmuir.5b02545.

[36]   Lukowicz T, Illous E, Nardello-Rataj V, Aubry J-M. Prediction of the equivalent alkane carbon number (EACN) of aprotic polar oils with COSMO-RS sigma-moments. Colloids Surf, A 2018;536:53–9. https://doi.org/10.1016/j.colsurfa.2017.07.068.

[37]   Tchakalova V, Testard F, Wong K, Parker A, Benczédi D, Zemb T. Solubilization and interfacial curvature in microemulsions: I. Interfacial expansion and co-extraction of oil. Colloids Surf, A 2008;331:31–9. https://doi.org/10.1016/j.colsurfa.2008.07.061.

[38]   Tchakalova V, Testard F, Wong K, Parker A, Benczédi D, Zemb T. Solubilization and interfacial curvature in microemulsions: II. Surfactant efficiency and PIT. Colloids Surf, A 2008;331:40–7. https://doi.org/10.1016/j.colsurfa.2008.07.060.

[39]   Shinoda K, Kunieda H. Phase properties of emulsions: PIT and HLB. Encyclopedia of Emulsion Technology 1983;1:337–67.

[40]   Förster T, Rybinski WV, Tesmann H, Wadle A. Calculation of optimum emulsifier mixtures for phase inversion emulsification. Int J Cosmet Sci 1994;16:84–92. https://doi.org/10.1111/j.1467-2494.1994.tb00086.x.

[41]   Wade WH, Morgan JC, Schechter RS, Jacobson JK, Salager JL. Interfacial tension and phase behavior of surfactant systems. Soc Pet Eng J 1978;18:242–52. https://doi.org/10.2118/6844-PA.

[42]   Graciaa A, Lachaise J, Sayous JG, Grenier P, Yiv S, Schechter RS, et al. The partitioning of complex surfactant mixtures between oil/water/microemulsion phases at high surfactant concentrations. J Colloid Interface Sci 1983;93:474–86. https://doi.org/10.1016/0021-9797(83)90431-9.

[43]   Arai H, Shinoda K. The effect of mixing of oils and of nonionic surfactants on the phase inversion temperatures of emulsions. J Colloid Interface Sci 1967;25:396–400. https://doi.org/10.1016/0021-9797(67)90047-1.

[44]   Shinoda K, Kunieda H. Conditions to produce so-called microemulsions: Factors to increase the mutual solubility of oil and water by solubilizer. J Colloid Interface Sci 1973;42:381–7. https://doi.org/10.1016/0021-9797(73)90303-2.

[45]   Reed RL, Healy RN. Some physicochemical aspects of microemulsion flooding: a review. Improved oil recovery by surfactant and polymer flooding. Academic Press, Shah, D. O.; Schechter R. S.; 1977, p. 383–437.

[46]   Salager J-L, Forgiarini AM, Marquez L, Manchego L, Bullon J. How to Attain an Ultralow Interfacial Tension and a Three-Phase Behavior with a Surfactant Formulation for Enhanced Oil Recovery: A Review. Part 2. Performance Improvement Trends from Winsor's Premise to Currently Proposed Inter- and Intra-Molecular Mixtures. J Surfactants Deterg 2013;16:631–63. https://doi.org/10.1007/s11743-013-1485-x.

[47]   Bourrel M, Salager JL, Schechter RS, Wade WH. A correlation for phase behavior of nonionic surfactants. J Colloid Interface Sci 1980;75:451–61. https://doi.org/10.1016/0021-9797(80)90470-1.

[48]   Ontiveros JF, Pierlot C, Catte M, Molinier V, Salager J-L, Aubry J-M. A simple method to assess the hydrophilic lipophilic balance of food and cosmetic surfactants using the phase inversion temperature of C10E4/n-octane/water emulsions. Colloids Surf, A 2014;458:32–9. https://doi.org/10.1016/j.colsurfa.2014.02.058.

[49]   Ontiveros JF, Pierlot C, Catte M, Molinier V, Salager J-L, Aubry J-M. Structure-interfacial properties relationship and quantification of the amphiphilicity of well-defined ionic and non-ionic surfactants using the PIT-slope method. J Colloid Interface Sci 2015;448:222–30. https://doi.org/10.1016/j.jcis.2015.02.028.

[50]   Burauer S, Sachert T, Sottmann T, Strey R. On microemulsion phase behavior and the monomeric solubility of surfactant. Phys Chem Chem Phys 1999;1:4299–306. https://doi.org/10.1039/a903542g.

[51]   Tolosa L-I, Forgiarini A, Moreno P, Salager J-Louis. Combined Effects of Formulation and Stirring on Emulsion Drop Size in the Vicinity of Three-Phase Behavior of Surfactant-Oil Water Systems. Ind Eng Chem Res 2006;45:3810–4. https://doi.org/10.1021/ie060102j.

[52]   Salager JL, Perez-Sanchez M, Garcia Y. Physicochemical parameters influencing the emulsion drop size. Colloid Polym Sci 1996;274:81–4. https://doi.org/10.1007/BF00658913.

[53]   Hirasaki G, Miller CA, Puerto M. Recent Advances in Surfactant EOR. Soc Pet Eng J 2011;16:889–907. https://doi.org/10.2118/115386-PA.

[54]   Ghosh S, Johns RT. An Equation-of-State Model To Predict Surfactant/Oil/Brine-Phase Behavior. Soc Pet Eng J 2016;21:1 106-1 125. https://doi.org/10.2118/170927-PA.

[55]   Chang L, Pope GA, Jang SH, Tagavifar M. Prediction of microemulsion phase behavior from surfactant and co-solvent structures. Fuel 2019;237:494–514. https://doi.org/10.1016/j.fuel.2018.09.151.

[56]   Creton B, Lévêque I, Oukhemanou F. Equivalent alkane carbon number of crude oils: A predictive model based on machine learning. Oil Gas Sci Technol 2019;74:30. https://doi.org/10.2516/ogst/2019002.

[57]   Kunieda H, Shinoda K. Phase behavior in systems of nonionic surfactant/ water/ oil around the hydrophile-lipophile-balance-temperature (HLB-temperature). J Dispersion Sci Technol 1982;3:233–44. https://doi.org/10.1080/01932698208943639.

[58]   Salager J-L, Forgiarini A, Marquez R. Extended Surfactants Including an Alkoxylated Central Part Intermediate Producing a Gradual Polarity Transition—A Review of the Properties Used in Applications Such as Enhanced Oil Recovery and Polar Oil Solubilization in Microemulsions. J Surfactants Deterg 2019;22:935–972. https://doi.org/10.1002/jsde.12331.

[59]   Salager J-L, Forgiarini AM, Bullon J. How to Attain Ultralow Interfacial Tension and Three-Phase Behavior with Surfactant Formulation for Enhanced Oil Recovery: A Review. Part 1. Optimum Formulation for Simple Surfactant-Oil-Water Ternary Systems. J Surfactants Deterg 2013;16:449–72. https://doi.org/10.1007/s11743-013-1470-4.

[60] Ontiveros JF, Pierlot C, Catte M, Salager J-L, Aubry J-M. Determining the Preferred Alkane Carbon Number (PACN) of nonionic surfactants using the PIT-slope method. Colloids Surf, A 2018;536:30–7. https://doi.org/10.1016/j.colsurfa.2017.08.002.

[61] Kahlweit M, Strey R, Haase D, Firman P. Properties of the three-phase bodies in water-oil-nonionic amphiphile mixtures. Langmuir 1988;4:785–90. https://doi.org/10.1021/la00082a001.

[62] Rosen MJ, Kunjappu JT. Surfactants and Interfacial Phenomena. John Wiley & Sons; 2012.

[63] Pizzino A, Molinier V, Catte M, Salager J-L, Aubry J-M. Bidimensional Analysis of the Phase Behavior of a Well-Defined Surfactant (C10E4)/Oil (n-Octane)/Water-Temperature System. J Phys Chem B 2009;113:16142–50. https://doi.org/10.1021/jp907261u.

[64] Saito H, Shinoda K. The stability of W/O type emulsions as a function of temperature and of the hydrophilic chain length of the emulsifier. J Colloid Interface Sci 1970;32:647–51. https://doi.org/10.1016/0021-9797(70)90158-X.

[65] Shinoda K. Solution behavior of surfactants: The importance of surfactant phase and the continuous change in HLB of surfactant. Prog Colloid Polym Sci 1983:1–7. https://doi.org/doi:10.1007/BFb0114132.

[66] Kunieda H, Friberg SE. Critical Phenomena in a Surfactant/Water/Oil System. Basic Study on the Correlation between Solubilization, Microemulsion, and Ultralow Interfacial Tensions. Bull Chem Soc Jpn 1981;54:1010–4. https://doi.org/10.1246/bcsj.54.1010.

[67] Kahlweit M, Strey Reinhard. Phase behavior of ternary systems of the type water-oil-nonionic amphiphiles (microemulsions). Angew Chem 1985;97:655–69.

[68] Kahlweit M, Strey R, Busse G. Effect of alcohols on the phase behavior of microemulsions. J Phys Chem 1991;95:5344–52. https://doi.org/10.1021/j100166a077.

[69] Blute I, Svensson M, Holmberg K, Bergh M, Karlberg A-T. Solution behaviour of a formate capped surfactant—the oxidation product of an alcohol ethoxylate. Colloids Surf, A 1999;160:229–36. https://doi.org/10.1016/S0927-7757(99)00188-0.

[70] Schubert KV, Strey R, Kahlweit M. A new purification technique for alkyl polyglycol ethers and miscibility gaps for water-CiEj. J Colloid Interface Sci 1991;141:21–9. https://doi.org/10.1016/0021-9797(91)90298-M.

[71] Schubert KV, Strey R, Kahlweit M. 3PHEX: a new surfactant purification technique. Prog Colloid Polym Sci 1991;84:103–6. https://doi.org/10.1007/BFb0115946.

[72] Zarate-Muñoz S, Troncoso AB, Acosta E. The Cloud Point of Alkyl Ethoxylates and Its Prediction with the Hydrophilic–Lipophilic Difference (HLD) Framework. Langmuir 2015;31:12000–8. https://doi.org/10.1021/acs.langmuir.5b03064.

[73] Kahlweit M, Lessner E, Strey R. Influence of the properties of the oil and the surfactant on the phase behavior of systems of the type water-oil-nonionic surfactant. J Phys Chem 1983;87:5032–40. https://doi.org/10.1021/j150642a051.

[74] Abillon O, Lee LT, Langevin D, Wong K. Microemulsions: Structures, surfactant layer properties and wetting transitions. Physica A (Amsterdam, Neth) 1991;172:209–18. https://doi.org/10.1016/0378-4371(91)90321-3.

[75] Kunieda H, Shinoda K. Evaluation of the hydrophile-lipophile balance (HLB) of nonionic surfactants. I. Multisurfactant systems. J Colloid Interface Sci 1985;107:107–21. https://doi.org/10.1016/0021-9797(85)90154-7.

[76] Tchakalova V, Fieber W. Classification of Fragrances and Fragrance Mixtures Based on Interfacial Solubilization. J Surfactants Deterg 2012;15:167–77. https://doi.org/10.1007/s11743-011-1295-y.

[77] Balogh J, Olsson U, Pedersen JS. Dependence on Oil Chain Length of the Curvature Elastic Properties of Nonionic Surfactant Films: Emulsification Failure and Phase

Equilibria. J Dispersion Sci Technol 2006;27:497–510. https://doi.org/10.1080/01932690500374250.

[78]   Kanei N, Tamura Y, Kunieda H. Effect of Types of Perfume Compounds on the Hydrophile–Lipophile Balance Temperature. J Colloid Interface Sci 1999;218:13–22. https://doi.org/10.1006/jcis.1999.6371.

[79]   Dörfler H-D. The influence of ethylene glycol on the phase behavior of aqueous microemulsions in quaternary systems. In: Lagaly G, editor. Horizons 2000 – aspects of colloid and interface science at the turn of the millenium, Steinkopff; 1998, p. 118–25.

[80]   Schneider K, Ott TM, Schweins R, Frielinghaus H, Lade O, Sottmann Thomas. Phase Behavior and Microstructure of Symmetric Nonionic Microemulsions with Long-Chain n-Alkanes and Waxes. Ind Eng Chem Res 2019;58:2583–95. https://doi.org/10.1021/acs.iecr.8b04833.

[81]   Lade O, Beizai K, Sottmann T, Strey R. Polymerizable Nonionic Microemulsions: Phase Behavior of H2O-n-Alkyl Methacrylate-n-Alkyl Poly(ethylene glycol) Ether (CiEj). Langmuir 2000;16:4122–30. https://doi.org/10.1021/la991232i.

[82]   Gu T, Sjöblom J. Surfactant structure and its relation to the Krafft point, cloud point and micellization: Some empirical relationships. Colloids and Surfaces 1992;64:39–46. https://doi.org/10.1016/0166-6622(92)80160-4.

[83]   John Mitchell D, T. Tiddy GJ, Waring L, Bostock T, P. McDonald M. Phase behaviour of polyoxyethylene surfactants with water. Mesophase structures and partial miscibility (cloud points). J Chem Soc, Faraday Trans 1 1983;79:975–1000. https://doi.org/10.1039/F19837900975.

[84]   Graciaa A, Anderez J, Bracho C, Lachaise J, Salager J-L, Tolosa L, et al. The selective partitioning of the oligomers of polyethoxylated surfactant mixtures between interface and oil and water bulk phases. Adv Colloid Interface Sci 2006;123–126:63–73. https://doi.org/10.1016/j.cis.2006.05.015.

[85]   Kunieda H, Yamagata M. Three-phase behavior in a mixed nonionic surfactant system. Colloid Polym Sci 1993;271:997–1004. https://doi.org/10.1007/BF00654860.

[86]   Os NM van, Haak JR, Rupert LAM. Physico-Chemical Properties of Selected Anionic, Cationic and Nonionic Surfactants. Elsevier; 1993.

[87]   Puvvada S, Blankschtein D. Theoretical and experimental investigations of micellar properties of aqueous solutions containing binary mixtures of nonionic surfactants. J Phys Chem 1992;96:5579–92.

[88]   Puvvada S, Blankschtein D. Molecular-thermodynamic approach to predict micellization, phase behavior and phase separation of micellar solutions. I. Application to nonionic surfactants. J Chem Phys 1990;92:3710–24. https://doi.org/10.1063/1.457829.

[89]   Suzuki T, Esumi K, Meguro K. The study of the micelle structure of nonionic surfactant by using a keto—enolic tautomerism. J Colloid Interface Sci 1983;93:205–14. https://doi.org/10.1016/0021-9797(83)90398-3.

[90]   Hinze WL, Pramauro E. A Critical Review of Surfactant-Mediated Phase Separations (Cloud-Point Extractions): Theory and Applications. Crit Rev Anal Chem 1993;24:133–77. https://doi.org/10.1080/10408349308048821.

[91]   Schubert K-V, Strey R, Kline SR, Kaler EW. Small angle neutron scattering near Lifshitz lines: transition from weakly structured mixtures to microemulsions. J Chem Phys 1994;101:5343–55. https://doi.org/10.1063/1.467387.

[92]   Fogden A, T. Hyde S, Lundberg G. Bending energy of surfactant films. Journal of the Chemical Society, Faraday Transactions 1991;87:949–55. https://doi.org/10.1039/FT9918700949.

[93]   Strey R. Microemulsion microstructure and interfacial curvature. Colloid Polym Sci 1994;272:1005–19. https://doi.org/10.1007/BF00658900.

[94]   Acosta EJ. The HLD–NAC equation of state for microemulsions formulated with nonionic alcohol ethoxylate and alkylphenol ethoxylate surfactants. Colloids Surf, A 2008;320:193–204. https://doi.org/10.1016/j.colsurfa.2008.01.049.

[95]   Do LD, Withayyapayanon A, Harwell JH, Sabatini DA. Environmentally Friendly Vegetable Oil Microemulsions Using Extended Surfactants and Linkers. J Surfactants Deterg 2009;12:91–9. https://doi.org/10.1007/s11743-008-1096-0.

[96]   Solans C, Kunieda H. Industrial Applications of Microemulsions. CRC Press; 1996.

[97]   Lukowicz T, Company Maldonado R, Molinier V, Aubry J-M, Nardello-Rataj Veronique. Fragrance solubilization in temperature insensitive aqueous microemulsions based on synergistic mixtures of nonionic and anionic surfactants. Colloids Surf, A 2014;458:85–95. https://doi.org/10.1016/j.colsurfa.2013.11.024.

[98]   Asua JM. Miniemulsion polymerization. Prog Polym Sci 2002;27:1283–346. https://doi.org/10.1016/S0079-6700(02)00010-2.

[99]   Bera A, Kumar T, Ojha K, Mandal A. Screening of microemulsion properties for application in enhanced oil recovery. Fuel 2014;121:198–207. https://doi.org/10.1016/j.fuel.2013.12.051.

[100]   Wan W, Zhao J, Harwell JH, Shiau B-J. Characterization of Crude Oil Equivalent Alkane Carbon Number (EACN) for Surfactant Flooding Design. J Dispersion Sci Technol 2016;37:280–7. https://doi.org/10.1080/01932691.2014.950739.

[101]   Castellino V, Cheng Y-L, Acosta E. The hydrophobicity of silicone-based oils and surfactants and their use in reactive microemulsions. J Colloid Interface Sci 2011;353:196–205. https://doi.org/10.1016/j.jcis.2010.09.004.

[102]   Bouton F. Influence of terpenes and terpenoids on the phase behavior of micro- and macro-emulsions. thesis. Lille 1, 2010.

[103]   Burauer S, Sottmann T, Strey R. Nonionic microemulsions with cyclic oils. Tenside, Surfactants, Deterg 2000;37:8–16.

[104]   Lukowicz T. Synergistic solubilisation of fragrances in binary surfactant systems and prediction of their EACN value with COSMO-RS. thesis. Lille 1, 2015.

[105]   Egger H, Sottmann T, Strey R, Valero C, Berkessel A. Nonionic microemulsions with chlorinated hydrocarbons for catalysis. Tenside, Surfactants, Deterg 2002;39:17–22.

[106]   Deen GR, Pedersen JS. Phase Behavior and Microstructure of C12E5 Nonionic Microemulsions with Chlorinated Oils. Langmuir 2008;24:3111–7. https://doi.org/10.1021/la703323n.

[107]   Wormuth KR, Kaler EW. Microemulsifying polar oils. J Phys Chem 1989;93:4855–61. https://doi.org/10.1021/j100349a035.

[108]   Kahlweit M, Busse G, Faulhaber B, Eibl H. Preparing nontoxic microemulsions. Langmuir 1995;11:4185–7. https://doi.org/10.1021/la00011a001.

[109]   Teixeira MA, Barrault L, Rodríguez O, Carvalho CC, Rodrigues AE. Perfumery Radar 2.0: A Step toward Fragrance Design and Classification. Ind Eng Chem Res 2014;53:8890–912. https://doi.org/10.1021/ie403968w.

[110]   Rondon M, Pereira JC, Bouriat P, Graciaa A, Lachaise J, Salager J-L. Breaking of Water-in-Crude-Oil Emulsions. 2. Influence of Asphaltene Concentration and Diluent Nature on Demulsifier Action. Energy Fuels 2008;22:702–7. https://doi.org/10.1021/ef7003877.

[111]   Ghayour A, Acosta E. Characterizing the Oil-like and Surfactant-like Behavior of Polar Oils. Langmuir 2019;35:15038–50. https://doi.org/10.1021/acs.langmuir.9b02732.

[112]   Gradzielski M, Langevin D, Sottmann T, Strey R. Droplet microemulsions at the emulsification boundary: The influence of the surfactant structure on the elastic constants of the amphiphilic film. J Chem Phys 1997;106:8232–8. https://doi.org/10.1063/1.473888.

[113]   Prévost S, Gradzielski M, Zemb T. Self-assembly, phase behaviour and structural behaviour as observed by scattering for classical and non-classical microemulsions. Adv Colloid Interface Sci 2017;247:374–96. https://doi.org/10.1016/j.cis.2017.07.022.

[114]   N. Israelachvili J, John Mitchell D, W. Ninham B. Theory of self-assembly of hydrocarbon amphiphiles into micelles and bilayers. J Chem Soc, Faraday Trans 2 1976;72:1525–68. https://doi.org/10.1039/F29767201525.

[115]   Tanford C. The hydrophobic effect: formation of micelles and biological membranes. Wiley; 1980.

[116]   Israelachvili JN. Intermolecular and Surface Forces. Academic Press; 2015.

[117]   Barnes IS, Hyde ST, Ninham BW, Derian PJ, Drifford M, Zemb TN. Small-angle x-ray scattering from ternary microemulsions determines microstructure. The Journal of Physical Chemistry 1988;92:2286–2293.

[118]   Sottmann T, Strey R, Chen S-H. A small-angle neutron scattering study of nonionic surfactant molecules at the water-oil interface: area per molecule, microemulsion domain size, and rigidity. J Chem Phys 1997;106:6483–91. https://doi.org/10.1063/1.473638.

[119]   Zemb T. Flexibility, persistence length and bicontinuous microstructures in microemulsions. Comptes Rendus Chimie 2009;12:218–224.

[120]   Requena J., Billett D. F., Haydon Denis Arthur. Van der Waals forces in oil–water systems from the study of thin lipid films - I. Measurement of the contact angle and the estimation of the van der Waals free energy of thinning of a film. Proc R Soc London, Ser A 1975;347:141–59. https://doi.org/10.1098/rspa.1975.0202.

[121]   Chen SJ, Evans DF, Ninham BW, Mitchell DJ, Blum FD, Pickup S. Curvature as a determinant of microstructure and microemulsions. J Phys Chem 1986;90:842–7. https://doi.org/10.1021/j100277a027.

[122]   Klamt A. Conductor-like Screening Model for Real Solvents: A New Approach to the Quantitative Calculation of Solvation Phenomena. J Phys Chem 1995;99:2224–35. https://doi.org/10.1021/j100007a062.

[123]   Buggert M, Cadena C, Mokrushina L, Smirnova I, Maginn EJ, Arlt W. COSMO-RS Calculations of Partition Coefficients: Different Tools for Conformation Search. Chem Eng Technol 2009;32:977–86. https://doi.org/10.1002/ceat.200800654.

[124]   Klamt A, Huniar U, Spycher S, Keldenich J. COSMOmic: A Mechanistic Approach to the Calculation of Membrane−Water Partition Coefficients and Internal Distributions within Membranes and Micelles. J Phys Chem B 2008;112:12148–57. https://doi.org/10.1021/jp801736k.

[125]   Klamt A, Schwöbel J, Huniar U, Koch L, Terzi S, Gaudin T. COSMOplex : self-consistent simulation of self-organizing inhomogeneous systems based on COSMO-RS. Phys Chem Chem Phys 2019;21:9225–38. https://doi.org/10.1039/C9CP01169B.

[126]   Klamt A. COSMO-RS: from quantum chemistry to fluid phase thermodynamics and drug design. 1. ed. Amsterdam: Elsevier; 2005.

[127]   Pleines M, Kunz W, Zemb T, Benczédi D, Fieber W. Molecular factors governing the viscosity peak of giant micelles in the presence of salt and fragrances. J Colloid Interface Sci 2019;537:682–93. https://doi.org/10.1016/j.jcis.2018.11.072.

[128]   Salager JL, Bourrel M, Schechter RS, Wade WH. Mixing rules for optimum phase-behavior formulations of surfactant/oil/water systems. Soc Pet Eng J 1979;19:271–8. https://doi.org/10.2118/7584-PA.

[129]   Salager JL, Anton RE. Physicochemical characterization of a surfactant. A quick and precise method. J Dispersion Sci Technol 1983;4:253–73. https://doi.org/10.1080/01932698308943370.

[130]   Baran JR, Pope GA, Wade WH, Weerasooriya V, Yapa A. Microemulsion Formation with Mixed Chlorinated Hydrocarbon Liquids. J Colloid Interface Sci 1994;168:67–72. https://doi.org/10.1006/jcis.1994.1394.

[131]   Szekeres E, Acosta E, Sabatini DA, Harwell JH. A Two-State Model for Selective Solubilization of Benzene−Limonene Mixtures in Sodium Dihexyl Sulfosuccinate Microemulsions. Langmuir 2004;20:6560–9. https://doi.org/10.1021/la036482k.

[132]   Ontiveros JF, Durand M, Pierlot C, Quellet C, Nardello-Rataj V, Aubry J-M. Dramatic influence of fragrance alcohols and phenols on the phase inversion temperature of the Brij30/n-octane/water system. Colloids Surf, A 2015;478:54–61. https://doi.org/10.1016/j.colsurfa.2015.03.051.

[133]   Stubenrauch C. Microemulsions: Background, New Concepts, Applications, Perspectives. Wiley; 2008.

[134]   Larcinese-Hafner V, Tchakalova V. Co-surfactant, co-solvent, and hydrotropic properties of some common cooling agents. Flavour Fragrance J 2018;33:303–12. https://doi.org/10.1002/ffj.3449.

$$HLD_N = PACN - EACN + \tau.(T-25)$$